

BEHAVIOR OF SHEAR
TEST STRUCTURE

R. C. Shilling
M. D. Vanderbilt

Structural Research Report No. 5
Civil Engineering Department
Colorado State University
Fort Collins, Colorado 80521

June, 1970



U18401 0575803

TABLE OF CONTENTS

| | Page |
|---|--------|
| List of Tables | vi |
| List of Figures | vii |
| Chapter | |
| 1 INTRODUCTION | 1 |
| 1.1 Object | 1 |
| 1.2 Scope | 1 |
| 1.3 Acknowledgments | 3 |
| 1.4 Notation | 3 |
| 2 DESCRIPTION OF TEST SPECIMEN | 5 |
| 2.1 Introductory Remarks | 5 |
| 2.2 The Elastic Specimen | 5 |
| 2.3 Design of Reinforced Concrete Test Specimen | 7 |
| 2.4 Materials | 9 |
| 2.5 Construction of Specimens | 10 |
| 3 BEHAVIOR | 13 |
| 3.1 Introductory Remarks | 13 |
| 3.2 Cracking | 13 |
| (a) Flexural Cracking | 13 |
| (b) Shear Cracking | 15 |
| 3.3 Deflections | 17 |
| 3.4 Mode of Failure | 18 |
| 3.5 Strength Discussion | 19 |
| (a) Flexural Strength | 19 |
| (b) Shear Strength | 19 |
| 4 SUMMARY AND CONCLUSIONS | 21 |
| 4.1 Summary | 21 |
| 4.2 Conclusions | 21 |
| BIBLIOGRAPHY | 23 |
| TABLES | 25 |
| APPENDIX A FLEXURAL STRENGTH ANALYSIS | 53 |
| A.1 Introductory Remarks | 54 |
| A.2 Analysis | 56 |

TABLE OF CONTENTS (Continued)

| | Page |
|---|------|
| A.3 Results | 60 |
| A.4 Computation of V_{flex} | 60 |

LIST OF TABLES

| Table No. | Page |
|--|------|
| 2.1 Mix Design | 25 |
| 3.1 Specimen Data | 26 |
| A.1 Comparison of Analyses with and without Corner Levers | 62 |

LIST OF FIGURES

| Figure No. | Page |
|--|------|
| 2.1 Lines of Contraflexure Around Point Support | 27 |
| 2.2 Proposed Specimen. | 28 |
| 2.3 Test Specimens. | 29 |
| 2.4 Steel Layout, 1% Negative | 30 |
| 2.5 Steel Layout, 2% Negative | 31 |
| 2.6 Beam Steel | 32 |
| 2.7 Typical Stress-Strain Curve, Batch No. 1 | 33 |
| 2.8 Typical Stress-Strain Curve, Batch No. 2 | 34 |
| 2.9 Formwork for Specimen | 35 |
| 2.10 Approximate Batch Locations | 36 |
| 3.1 Crack Pattern, Specimen 2S2 - 7 | 37 |
| 3.2 Crack Pattern, Specimen 6C1 - 9 | 38 |
| 3.3 Crack Pattern, Specimen 4C1 - 12 | 39 |
| 3.4 Crack Pattern, Specimen 6S2 - 14. | 40 |
| 3.5 Crack Detectors in Place | 41 |
| 3.6 Load vs. Strain in Crack Detector Gages | 42 |
| 3.7 Load vs. Strain in Crack Detector Gages | 43 |
| 3.8 Load vs. Strain in Crack Detector Gages | 44 |
| 3.9 Dial Gage Location and Setup | 45 |
| 3.10 Load vs. Deflection, $r/d = 2$ | 46 |
| 3.11 Load vs. Deflection, $r/d = 3$ | 47 |
| 3.12 Load vs. Deflection, $r/d = 4$ | 48 |
| 3.13 Load vs. Deflection, $r/d = 6$ | 49 |
| 3.14 Load vs. Deflection, $r/d = 8$ | 50 |
| 3.15 Comparison of Elastic Analysis and Test Specimens, Load vs. Deflection | 51 |
| 3.16 $v_u / \sqrt{f'_c}$ vs. r/d | 52 |
| A.1 Yield-Line Analysis of Uniformly Loaded, Simply Supported Slab | 63 |
| A.2 Yield-Line Pattern. | 64 |
| A.3 Variation of QL^2 with r/L | 65 |
| A.4 Variation of α with r/l | 66 |

CHAPTER 1

INTRODUCTION

1.1 Object

The shear strength of flat plate reinforced concrete floor systems has been the subject of numerous investigations (4, 7, 9, 10, 14, 15, 16, 17, 18)* and a multitude of equations for predicting ultimate strength in shear have been developed. While any given empirical equation provides a reasonable fit to the data used in developing that equation, no universally applicable equation for calculating the shear strength has been found.

The objective of this investigation was to add to the information already available by tests and analyses of a new type of specimen which more closely simulates the structural action of continuous multi-panel slabs than specimens previously utilized. The behavior of the specimens up to failure was investigated, and the chief result sought was a better understanding of the behavior and strength characteristics of continuous flat plate structures.

1.2 Scope

This investigation included the construction and testing to failure of 15 reinforced concrete test specimens. The behavior of

*Numbers in parentheses refer to entries in the bibliography.

the specimens during loading was observed, and an analysis of the test data was made. An elastic analysis of the specimens was also made.

The test specimens were assumed to more accurately represent the area inside the line of contraflexure around the column of an interior panel of a flat plate floor system than have the specimens of previous investigations. This assumption is discussed in Chapter 2. These specimens all consisted of a 9.5' x 9.5' square two inch thick slab, surrounded by a rigid edge beam, and having a column stub of variable size and shape at the center. The specimens were supported by point supports at the four corners and under the center column stub. Test variables included the reinforcement ratio, the ratio of column size to effective depth of slab (r/d), and column shape, either round or square. A description of the design and construction of the specimens is given in Chapter 2.

Chapter 3 contains a report on and discussion of the behavior of the specimens with respect to deflections, cracking, and mode of failure, as well as a discussion of the specimen strengths as compared to the flexural capacities computed by the yield-line method. The summary and conclusions are contained in Chapter 4. Appendix A represents a discussion of the yield-line analysis used to obtain the flexural strengths of the specimens. The analyses of the test data are given in a parallel report by Ford (5), while the elastic analyses are given in another report by Janowski (11).

1.3 Acknowledgments

This report was prepared as a Master's Thesis under the direction of Dr. M. D. Vanderbilt, Associate Professor of Civil Engineering. The investigation was supported by a grant from the National Science Foundation and was conducted at the Engineering Research Center Structural Laboratory of Colorado State University.

1.4 Notation

The symbols used in this report are defined below and where first introduced in the text.

b = perimeter of the column.

d = effective depth of slab steel = 1.5 inches.

f = coefficient taken from elastic analysis to be multiplied by M_{cr} to obtain q_{cr} .

f_c = compression cylinder strength of concrete.

f_r = modulus of rupture taken as $7.5\sqrt{f_c}$.

f_y = yield stress of reinforcing steel.

L = distance from center of column to center of edge beam in test specimens.

M_{cr} = moment at which first cracking occurs.

p = ratio of area of reinforcing steel to area of concrete for a unit width of slab.

q_{cr} = uniformly distributed load at which first cracking occurs.

q_{flex} = uniformly distributed load at which flexural failure occurs.

q_{test} = uniformly distributed load at which test specimen fails.

r = one-fourth the perimeter of the column.

S = section modulus for unit width of slab.

V_u = load on center column at which test specimen fails.

$v_u = V_u / bd.$

ψ = shear crack slope.

Notation which is used only in the appendix is defined in section A. 1.

CHAPTER 2

DESCRIPTION OF TEST SPECIMEN

2.1 Introductory Remarks

A total of fifteen specimens were constructed and tested to failure. The variables in the test program were the percent of reinforcement in the slab, the r/d ratio, or ratio of column size to effective depth of reinforcement, and the column shape, either square or circular.

The test specimen was assumed to represent the region of a multi-panel flat plate system around an interior column. This assumption is discussed in Section 2.2.

The design of the specimens is described in Section 2.3. The properties of the materials used are discussed in Section 2.4, and the method of construction of specimens in 2.5.

2.2 The Elastic Specimen

In previous test programs on punching shear in reinforced concrete slabs, some shape of the line of contraflexure for principal moments around a column in an interior panel of a flat plate structure was assumed. Simply supported plates of this shape were then tested and assumed to represent this portion of the panel.

These shapes, however, usually failed to adequately represent the structural behavior of a real interior panel since the boundary conditions for shear, deflection, and in-plane forces present in a real structure were absent or represented incorrectly in the test specimens. The previous specimens more nearly resembled footings than continuous slabs.

A new type of test specimen was proposed by Mowrer and Vanderbilt (17) that would eliminate these objections. The specimen was developed on the basis of elastic analyses of both continuous multipanel plates and isolated specimens. For a continuous structure composed of identical, uniformly loaded, square panels on identical square supports the line of contraflexure for principal moments is shown in Fig. 2. 1a. The line of contraflexure is of irregular shape and lies at about one-sixth of the span from the column face, regardless of support size (17).

Fig. 2. 1b shows the lines of contraflexure for principle moments for an isolated flat plate with clamped edges supported by a column in the center. The lines of contraflexure from Fig. 2. 1a are also superimposed on this figure. It can be seen that the lines of contraflexure around the column are very close in the two systems, with respect to shape, and with respect to position.

Based on the close correspondence between lines of contraflexure the isolated elastic plate was assumed to represent the

structural behavior of the continuous flat plate. The reinforced concrete specimen shown in Fig. 2.2 was then designed to model the elastic isolated plate with clamped edges. The specimen is a square plate surrounded by a rectangular edge beam, with a column at the center. There are point supports at the four corners and beneath the column. The specimens actually tested did not have the portion of the column which extends above the slab (Fig. 2.3).

Based on elastic analyses (2) it was expected that a rectangular edge beam of the size shown would have sufficient rigidity to closely simulate a clamped edge. Janowski (11) showed in the analytical phase of the study that this was not quite the case. Due to deflection and torsion of the edge beams, the line of contraflexure is located at a distance of about $L/4$ from the column face for the elastic structure rather than the $L/6$ shown in Fig. 2.1. While the behavior of the structure in the elastic range was not quite what was desired, the test specimen does represent a continuous structure more closely than any of the previous, "footing type" specimens tested in the past.

2.3 Design of Reinforced Concrete Test Specimen

The test specimens consisted of a two inch thick plate 9.5 feet square supported by an edge beam nine inches deep and six inches wide. At the center was a column of variable size and

shape (Fig. 2.3). The variables considered were column size and shape, and the amount of steel reinforcement.

A preliminary analysis of the elastic model showed the required locations of positive and negative moment reinforcement in orthogonal directions. Slabs were built with negative reinforcement over the center column amounting to either one or two percent reinforcement. The positive steel was one-half the percent of negative steel in either case. The negative steel framing into the spandrel beam was maintained at a constant one percent ratio. The percent of negative reinforcement for each specimen is shown in Table 3.1. The steel used is described in Section 2.4. The layouts of the two steel patterns are shown in Figs. 2.4 and 2.5.

The identifying numbers on each slab indicates the r/d ratio, shape of column, percent of negative reinforcement, p , and testing sequence. For example the identifying number 2S1 - 1 would indicate that this specimen had an r/d ratio of two, a square column, one percent negative reinforcement, and was the first specimen tested. The mark 3C1 - 4 would mean an r/d ratio of three, a round column, one percent negative steel, and the fourth test.

Beam reinforcement for the first specimen tested (2S1 - 1) consisted of No. 3 deformed bars as shown in Fig. 2.6a. Due to the development of large diagonal tension cracks in the edge beams of specimen 2S1 - 1, specimen number 3S1 - 2 was reinforced as

shown in Fig. 2.6b. Large deflections and torsions of the edge beams led to the further reinforcement of specimens 4S1 - 3 and 3C1 - 4 as shown in Fig. 2.6c and 6S1 - 5 through 4C2 - 15 as shown in Fig. 2.6d.

Center column reinforcement in specimens 2S1 - 1 and 3S1 - 2 consisted of No. 2 bars with hooks at the top which extended into the slab for two inches parallel to the slab steel. Specimens 2S2 - 7 and 2C1 - 11 had four vertical, unbent No. 2 bars, and all other specimens had four No. 3 bars, vertical and unbent, with two square No. 2 ties.

2.4 Materials

The concrete was mixed using one-half inch maximum size aggregate, because of small clearances, and sand having a fineness modulus of 2.75. Ideal brand, Type III portland cement was used in the mix.

The concrete was designed for a 7 day compressive cylinder strength (f'_c) of 3000 psi and a slump of six to eight inches (6). This high slump was to allow for better flow through the small clearances left by the thin slab.

Three different mix designs were used as shown in Table 2.1. Mix number one was used for specimen 2S1 - 1, mix number two for specimen 3S1 - 1, and mix number three for all subsequent specimens, except that, in some cases, very small amounts of

water were added to increase the slump. Cylinder strengths for the various slabs are shown in Table 3.1.

The slab reinforcement consisted of No. 2 deformed bars rolled by the Ziegler Steel Company of Los Angeles. Two batches were obtained, one with a yield stress of 44 ksi and the other of 56 ksi.

One bar from the first batch was cut into several pieces and one piece was tested each month or two for a period of one year to determine if the strength was time dependent. No time dependency was found, although the length of the yield plateau varied considerably among specimens. Typical load-strain curves for each batch are shown in Fig. 2.7 and 2.8.

For slabs 8S1 - 6 through 4C2 - 15 a piece of each bar used in the center negative mat was tested for its yield stress, and the average of all pieces was used in flexural strength calculations. These values are shown in Table 3.1.

The steel used in the beams was ASTM A-432 (60 ksi nominal) grade. The longitudinal steel consisted of No. 6 bars with a measured yield stress (f_y) of 65 ksi and the closed stirrups were No. 3 bars with a measured f_y of 73 ksi.

2.5 Construction

Fifteen specimens were constructed, with column size, shape, and percent of negative reinforcement as the variables. No

slab shear reinforcement was used. The beams were overreinforced to maintain their strength after cracking. The variables for each specimen are listed in Table 3.1.

The reinforcement was tied in mats and placed in the form on commercially produced metal chairs and tied down to prevent movement during casting. The top bars in the center negative mat were laid N-S in all slabs except for specimens 2S1 - 1 and 4S1 - 3. Care was taken in setting the bars on the form to maintain an effective depth of 1.5 inches to the plane of contact between the top and bottom layers of bars.

The bottom part of the form was made of 3/4 inch, plastic faced, form plywood on a framework of 2 x 4 lumber, and set on legs at a height of two feet above ground to permit tying down the rebar mats. The sides of the form were 9 inch channels set on edge and bolted together. The inner part of the form, which formed the inside upper face of the beams, was made of 3½ inch angles (Fig. 2.9). The form for the columns had to be remade for each specimen, and set in the center of the form. The junction between the column form and the main form was smoothed with plastic wood to ensure an even junction on the finished specimen.

Concrete batches were proportioned by weighing. The coarse aggregate and sand were placed in the mixer by conveyor belt, and the cement by hand. Water was metered in through a fitting in the

lid of the mixer. Six batches at six cubic feet per batch were required for each specimen. Slump tests were run on each batch, and one cylinder was taken from each batch except that six cylinders were taken from the last batch which always formed the column and the portion of the slab adjacent to the column and extending to the end of the interior negative slab steel. Approximate batch locations are shown in Fig. 2.10.

After casting, the slab portion was screeded to the desired 2 inch thickness. The screed rail was then removed, and the resulting trough filled and smoothed. When appropriate, finish trowelling was performed.

One inch thick square plates, with hemispherical holes in the bottom, were cast in the bottom of the column and the four corners of the beams to form support receptacles for the test stand. Three-eighth inch diameter bolts were cast vertically, and extending from the corners, for lifting purposes.

In addition, in slabs 6S1 - 5 through 4C2 - 15, one-fourth inch holes were provided on the south side and southwest corner of the columns, at a distance of one inch from the periphery, for the purpose of measuring the shear crack during testing (Fig. 2.3).

Specimens were cured in the form for at least seven days before testing. Details of the test setup, instrumentation, and testing procedure are described elsewhere (5).

CHAPTER 3

BEHAVIOR

3.1 Introductory Remarks

The test specimens were examined to determine their crack patterns, their load versus deflection behavior, and their modes of failure. These aspects of behavior were then correlated where possible with the information obtained from the elastic analyses by Janowski (11). Cracking is discussed in Section 3.3. Modes of failure are discussed in Section 3.4

A discussion of the specimen strengths is given in Section 3.5. This discussion includes a comparison with the flexural capacities as computed by the yield-line method described in Appendix A.

3.2 Cracking

(a) Flexural Cracking

As each specimen was tested, the bottom surface was examined for cracks at various load increments, and cracks were marked using an identifying symbol for that load increment.

Examination was done with a seven power, illuminated, magnifying lens. After testing, each slab was removed from the test stand, the bottom was photographed, and the specimen was discarded.

Figures 3.1 through 3.4 show photographs of typical specimens. The sequence of crack formation was as follows. First, tangential cracks parallel to the edge beams formed at slightly more than half the span from the column face to the edge beam. Next, more tangential cracks appeared until they covered an area from approximately 1.5 feet from the edge beam to approximately 1.5 feet from the column center. The next step was the formation of radial cracks along the diagonal lines of symmetry, followed by radial cracking all the way around the column, except for specimens 2S1 - 1 and 3S1 - 2 for which cracking extended along centerlines through the beams indicating an insufficiency of beam reinforcement.

The elastic analyses (11) showed the line of maximum positive principal moment to be closely a circle with a radius of approximately three feet from the column center for all specimens. First positive cracking usually was detected at about 1.0 psi for the specimens with smaller r/d ratios, and at higher loads (1.5 to 2.0 psi) for higher r/d ratios. In both cases, first positive flexural cracking usually appeared in lines on both sides of the line of maximum moment.

Loads corresponding to first cracking around the column and to first cracking along the line of maximum positive principal moments were computed using the results of the analyses performed by Janowski (11). The cracking moment was computed as

$$M_{cr} = Sf_r \quad (3.1)$$

where M_{cr} is the cracking moment,

S is the section modulus per unit width, and

f_r is the modulus of rupture taken as $7.5\sqrt{f'_c}$. (1)

The cracking load was then computed from the cracking moment using the relationship

$$q_{cr} = fM_{cr} \quad (3.2)$$

where q_{cr} = the uniformly distributed load at which first cracking occurs,

f = a coefficient taken from the elastic analyses.

The theoretical load corresponding to first negative cracking was about 0.26 psi for all slabs while the load for first positive cracking was about 1.18 psi for all slabs.

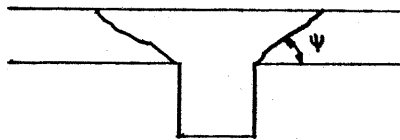
The basic cracking pattern was the same for all specimens. Specimens 6C1 - 9 and 8C1 - 13 however, developed wide torsional cracks along the edge beams. This pattern closely resembles the pattern used in the yield-line analysis of Appendix A.

(b) Shear Cracking

To measure the opening of the shear crack around the column, a "crack detector" was placed one inch out from the center of the west side of the column, and another one inch out along the

diagonal from the south-west corner on specimens 8S1 - 6 through 4C2 - 15 (Fig. 2.3 and 3.5). Specimen 6S1 - 5 had crack detectors on the east and west sides of the column, but none adjacent to the corner. The data obtained for specimens 8S1 - 6, 2S2 - 7 and 6C1 - 9 however, were not useable. Plots of strain in the gages on the crack detector vs. load on the slab for the remaining specimens are shown in Fig. 3.6 through 3.8. The data tend to show that shear cracks began opening at about 2.5 psi for specimens having an r/d ratio of four or less, and at about 3.5 psi for specimens with an r/d ratio of six or eight. Cracks opened first at the column corners, except in specimens 4S2 - 8 and 6S2 - 14. The shear cracks began opening rapidly just prior to failure, and this information was useful in predicting when the specimen would fail.

After testing the load apparatus was removed, the broken concrete was chipped away from around the column, and the shear crack slope (ψ) was measured. These slopes showed a range of 25° to 53° with an average of 36° as shown in sketch A. Moe (16) reported a slope of approximately 45° , while Mowrer (17) reported a slope of approximately 25° .



Sketch A

3.3 Deflections

Deflections were measured with dial gages placed on an E-W line of symmetry and on a diagonal line of symmetry as shown in Fig. 3.9. The gages were read after the application of each load increment.

Load vs. deflection curves are shown in Figs. 3.10 through 3.14 for a point two feet from the edge beam on the E-W line of symmetry which was the point of maximum measured deflection on this line. The specimens in the figures are grouped according to their r/d ratio. Specimens 4S2 - 8, 8S2 - 10 and 4C2 - 15 were unloaded during testing and this is shown in their respective curves.

In order to compare the deflections of the test specimens with those of the elastic analyses, the results from the latter for the same point on the slab are also plotted in Fig. 3.15a as straight lines labeled "elastic". Due to computer limitations the elastic analyses could not always be made for r/d ratios exactly corresponding to those used in the experimental phase of the study. Therefore the straight lines labeled "elastic" in Fig. 3.13 and 3.15b are for an r/d ratio of 5.3 instead of six. In plotting the results of the elastic analyses Young's modulus of 3.0×10^6 psi and Poisson's ratio of 0.15 were used.

It can be seen that the specimens remained essentially elastic to about 0.4 psi load. The cracking loads computed on the

basis of maximum negative moments obtained from the elastic analyses averaged about 0.26 psi. The specimens apparently remained "elastic" until the negative cracks formed all the way around the column.

An inability to correctly estimate Young's modulus could account for the fact that the test curves do not exactly coincide with the elastic curves for low loads.

3.4 Modes of Failure

Since all of the specimens ultimately failed by punching through of the column, the possibility of any "pure" flexural failures is ruled out immediately.

The load vs. deflection curves and the extensive cracking prior to failure indicate that all specimens failed in flexural-shear which is here defined as a punching shear failure preceded by extensive flexural cracking and pronounced deflections. The load vs. deflection curves showed a general loss of elasticity at about 0.4 psi, and an increasing rate of deflection with each load increment beyond this point, although the typical flat "plateau" indicative of flexural failure was never reached. Since the stress-strain curves for the No. 2 reinforcing exhibited only a very short yield plateau, no flat topped deflection curve was obtained.

3.5 Strength Discussion

(a) Shear Strength

Shown in Fig. 3.16 is a dimensionless plot of $v_u / \sqrt{f'_c}$ versus r/d where

$$v_u = V_u / bd,$$

V_u = the load on the center column at punching failure, and

b = perimeter of column.

As may be seen in Fig. 3.16 the unit shear strength for the square columns tends to decrease rather rapidly as r/d increases from two to four while the decrease is less rapid as r/d increases from four to eight. This may be attributed in part to the "damping out" of the effects of the stress concentrations at column corners with increase in r/d ratio (11).

The strength of circular columns is greater than that of square columns having identical r/d and reinforcement ratios. At least for intermediate ranges of r/d shear strength may be obtained more efficiently by changing shape than by increasing steel.

(b) Flexural Strength

The flexural capacities of all specimens were computed using the yield-line theory as presented in Appendix A. Shown in Table 3.1 are the values of uniform load, q_{flex} , obtained through the yield-line analysis, and the

portion of the yield load assigned to the center column, V_{flex} . Also given are ratios of q_{test}/q_{flex} . In general, for the same r/d , this ratio is considerably lower for the specimens with two percent steel than for one percent steel. There is also a trend towards a higher q_{test}/q_{flex} ratio as the r/d ratio goes up. The specimens with the lowest values of q_{test}/q_{flex} generally had the lowest deflections at failure as was expected. As shown in Table 3.1 all of the q_{test}/q_{flex} values were less than unity indicating that the specimens were in general not close to a flexural failure when they failed in shear. As shown in Fig. 3.10 and 3.14 the load deflection curves for all specimens were still increasing at failure as would be expected.

CHAPTER 4

SUMMARY AND CONCLUSIONS

4.1 Summary

This report describes the construction and testing to failure of fifteen reinforced concrete shear test specimens of a new type. All specimens consisted of a two inch thick slab, 9.5 feet square, surrounded by a 6" X 9" edge beam, and having a column cast monolithically in the center on one side. The variables were percent of steel, size of column, and shape of column, either square or round. A complete description of the specimens and their construction is given in Chapter 2.

All of the specimens failed in flexural-shear, a mode of failure defined as a punching shear failure preceded by extensive cracking and large deflections. A complete description of the behavior of the specimens with respect to cracking, deflections, modes of failure, and flexural vs. shear strength is given in Chapter 3.

4.2 Conclusions

The testing of this new type of specimen has added to the data on shear strength of reinforced concrete structures. The flexural

strength calculations served to illustrate the difficulty in using the shear strength equation developed by Moe, and the many derivatives of this equation. It was necessary to use test data in calculating V_{flex} , and this information is not usually available in an ordinary design situation.

Based on the results of this investigation, the following conclusions were reached:

1. The positive cracking pattern was in good qualitative agreement with the pattern used in the yield-line analysis, and with the location of the line of maximum positive moments as found in the elastic analyses.
2. A comparison of the load-deflection curves for a point on the specimen, with the results of the elastic analyses, indicates that the specimens departed from elastic behavior at 0.4 psi.
3. Dimensionless plots of shear strength vs. r/d ratio show that slabs with circular columns are stronger in shear than slabs with square columns having the same r/d ratio and percent of reinforcement. This is apparently due to the absence of stress concentrations around the circular columns which occur at the corners of square columns.

BIBLIOGRAPHY

1. American Concrete Institute, "ACI Standard Building Code Requirements for Reinforced Concrete", The Institute, Detroit, 1963.
2. Appleton, J. H., "Reinforced Concrete Floor Slabs on Flexible Beams", Illinois University Department of Civil Engineering, Structural Research Series No. 223, Urbana, Illinois, December, 1961.
3. Beedle, L. S., "Plastic Design of Steel Frames", John Wiley and Sons, Inc., New York, 1958.
4. Elstner, R. C., and Hognestad, E., "Shearing Strength of Reinforced Concrete Slabs", American Concrete Institute, Journal, 28:29 - 58, July, 1956.
5. Ford, R. O., "Analysis of Shear Test Structure", Colorado State University, Fort Collins, Colorado, 1970, (Master's Thesis).
6. Goldbeck, A. T., and Gray, J. E., "A Method of Proportioning Concrete for Strength, Workability, and Durability," National Crushed Stone Association, Engineering Bulletin No. 11, Washington, August, 1968.
7. Grow, J. B., and Vanderbilt, M. D., "A Study of the Shear Strength of Lightweight Prestressed Concrete Flat Plates", Colorado State University, Civil Engineering Department, Structural Research Report No. 2, Fort Collins, Colorado, December, 1966.
8. Hoff, N. J., "The Analysis of Structures", John Wiley and Sons, Inc., New York, 1964.
9. Hognestad, E., Elstner, R. D., and Hanson, J., "Shear Strength of Reinforced Structural Lightweight Aggregate Concrete Slabs", American Concrete Institute, Journal, 61:643 - 56, June, 1964.

10. Janney, R. , "Shear Strength of Flat Plate-Column Connections in Reinforced Concrete", Colorado State University, Fort Collins, Colorado, 1964, (Master's Thesis).
11. Janowski, R. H. , Jr. , "Elastic Analysis of Shear Test Plate", Colorado State University, Fort Collins, Colorado, 1970, (Master's Thesis).
12. Johansen, K. W. , "Yield Line Theory", Cement and Concrete Association, London, 1962, (Translation from Danish).
13. Jones, L. I. , and Wood, R. H. , "Yield-Line Analysis of Slabs, Thames & Hudson, Chatto & Windus, London, 1967.
14. Kinnunen, S. , and Nylander, H. , "Punching of Concrete Slabs Without Shear Reinforcement," Swedish Royal Institute of Technology, Transactions, No. 158, Stockholm, 1963.
15. Kinnunen, S. , "Punching of Slabs With Two-Way Reinforcement With Special Reference to Dowel Effect and Deviation of Reinforcement From Polar Symmetry", Swedish Royal Institute of Technology, Transactions No. 298, Stockholm, 1963.
16. Moe, J. , "Shearing Strength of Reinforced Concrete Slabs and Footings Under Concentrated Loads", Portland Cement Association Research and Development Laboratories, Development Department, Bulletin D47, Skokie, Illinois, April, 1961.
17. Mowrer, R. D. , and Vanderbilt, M. D. , "A Study of the Shear Strength of Lightweight Reinforced Concrete Flat Plates", Colorado State University, Civil Engineering Department, Structural Research Report No. 1, Fort Collins, Colorado, August, 1966.
18. Yitzhaki, D. , "Punching Strength of Reinforced Concrete Slabs", American Concrete Institute, Journal, 63:527 - 40, May, 1966.

TABLES

| <u>Ingredient</u> | <u>Mix No. 1</u> | <u>Mix No. 2</u> | <u>Mix No. 3</u> |
|---------------------|------------------|------------------|------------------|
| Cement | 96 lbs. | 115 lbs. | 115 lbs. |
| Fine Aggregate | 249 lbs. | 309 lbs. | 299 lbs. |
| Coarse Aggregate | 296 lbs. | 367 lbs. | 356 lbs. |
| Water | 8.7 gals. | 7.8 gals. | 10.4 gals |

Quantities shown are per six cubic foot batch.

Table 2.1. Mix Designs

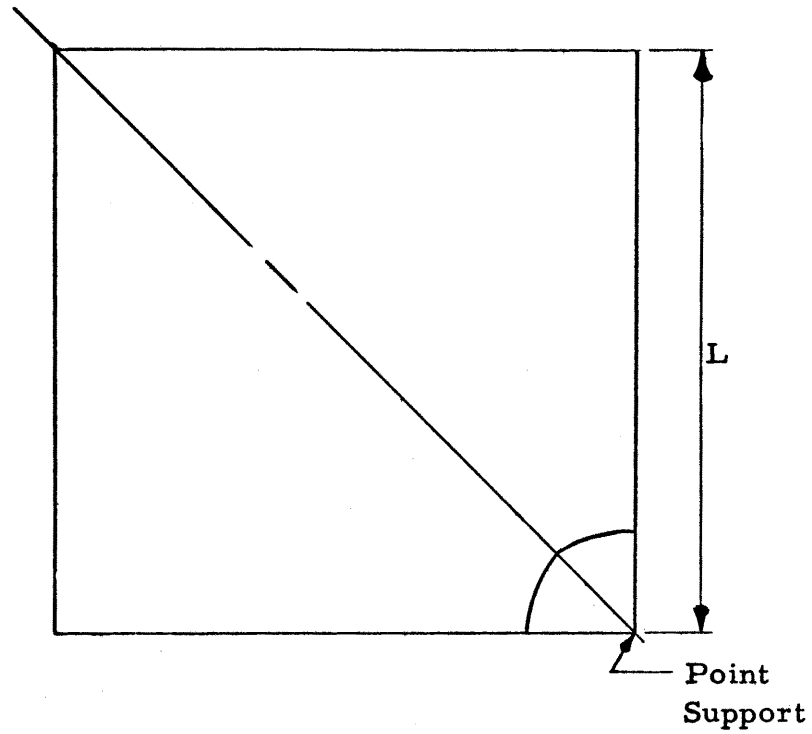
| MARK | r* (in.) | $\frac{r}{d}$ | f'_c (psi) | f_r^{**} (psi) | f_y (ksi) | p^- | v_u (psi) | $\frac{v_u}{f'_c}$ | V_u (ksi) | q_{flex} (psi) | $\frac{q_{test}}{q_{flex}}$ | V_{flex} (kips) |
|----------|-------------|---------------|-----------------|---------------------|----------------|-------|----------------|--------------------|----------------|---------------------|-----------------------------|----------------------|
| 2S1 - 1 | 3 | 2 | 4000 | 474 | 43.9 | .0098 | 536 | 8.49 | 9.65 | 6.31 | .397 | 24.4 |
| 3S1 - 2 | 4.5 | 3 | 3330 | 432 | 43.9 | .0098 | 388 | 6.72 | 10.48 | 6.37 | .392 | 26.7 |
| 4S1 - 3 | 6 | 4 | 3010 | 412 | 43.0 | .0098 | 321 | 5.85 | 11.54 | 6.32 | .464 | 25.0 |
| 3C1 - 4 | 4.5 | 3 | 3200 | 423 | 43.0 | .0098 | 487 | 8.61 | 13.13 | 6.22 | .518 | 25.3 |
| 6S1 - 5 | 9 | 6 | 3070 | 415 | 43.0 | .0098 | 326 | 5.89 | 17.60 | 6.59 | .662 | 26.6 |
| 8S1 - 6 | 12 | 8 | 2970 | 408 | 42.8 | .0098 | 282 | 5.16 | 20.28 | 6.81 | .645 | 31.4 |
| 2S2 - 7 | 3 | 2 | 3370 | 435 | 46.1 | .0196 | 619 | 10.68 | 11.13 | 9.69 | .258 | 43.1 |
| 4S2 - 8 | 6 | 4 | 3130 | 419 | 59.6 | .0196 | 432 | 7.67 | 15.54 | 12.21 | .269 | 57.7 |
| 6C1 - 9 | 18.83 | 5.88 | 3730 | 457 | 56.8 | .0098 | 409 | 6.68 | 21.63 | 8.56 | .565 | 38.5 |
| 8S2 - 10 | 12 | 8 | 3810 | 464 | 56.1 | .0196 | 356 | 5.77 | 25.65 | 13.19 | .395 | 65.0 |
| 2C1 - 11 | 3 | 2 | 2890 | 402 | 56.0 | .0098 | 487 | 9.07 | 8.77 | 7.58 | .298 | 29.4 |
| 4C1 - 12 | 6.07 | 4.04 | 3220 | 425 | 56.1 | .0098 | 448 | 7.90 | 16.30 | 8.09 | .464 | 34.3 |
| 8C1 - 13 | 11.89 | 7.91 | 3480 | 442 | 56.0 | .0098 | 318 | 5.40 | 22.68 | 8.79 | .579 | 39.3 |
| 6S2 - 14 | 9 | 6 | 2990 | 410 | 57.5 | .0196 | 334 | 6.10 | 18.01 | 12.23 | .321 | 56.2 |
| 4C2 - 15 | 6.08 | 4.04 | 3120 | 418 | 55.0 | .0196 | 595 | 10.65 | 21.70 | 11.49 | .413 | 52.5 |

* $r = \frac{1}{4}$ Column Periphery

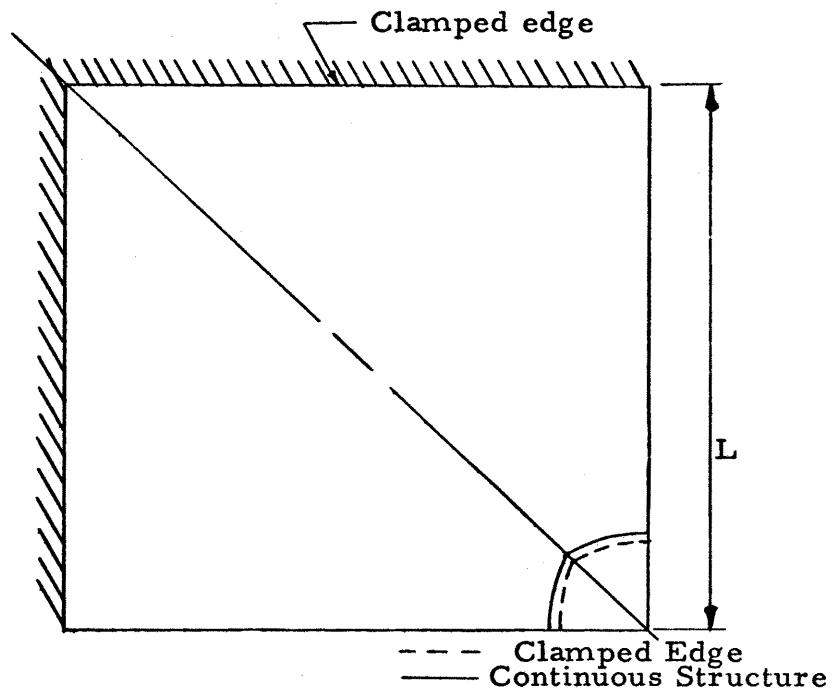
$$** f_r = 7.5 \sqrt{f'_c}$$

Table 3.1. Specimen Data

FIGURES



a. One-Fourth of one Panel of a Continuous Structure



b. One-Fourth of Clamped Edge Specimen

Fig. 2.1. Lines of Contraflexure Around Point Support

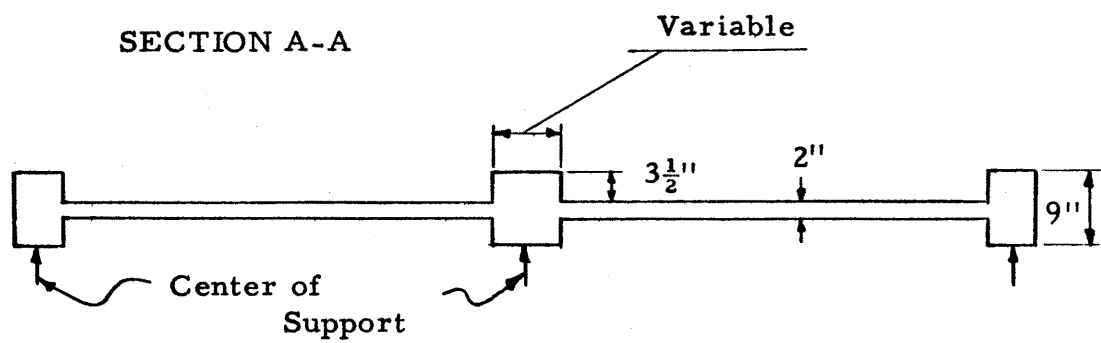
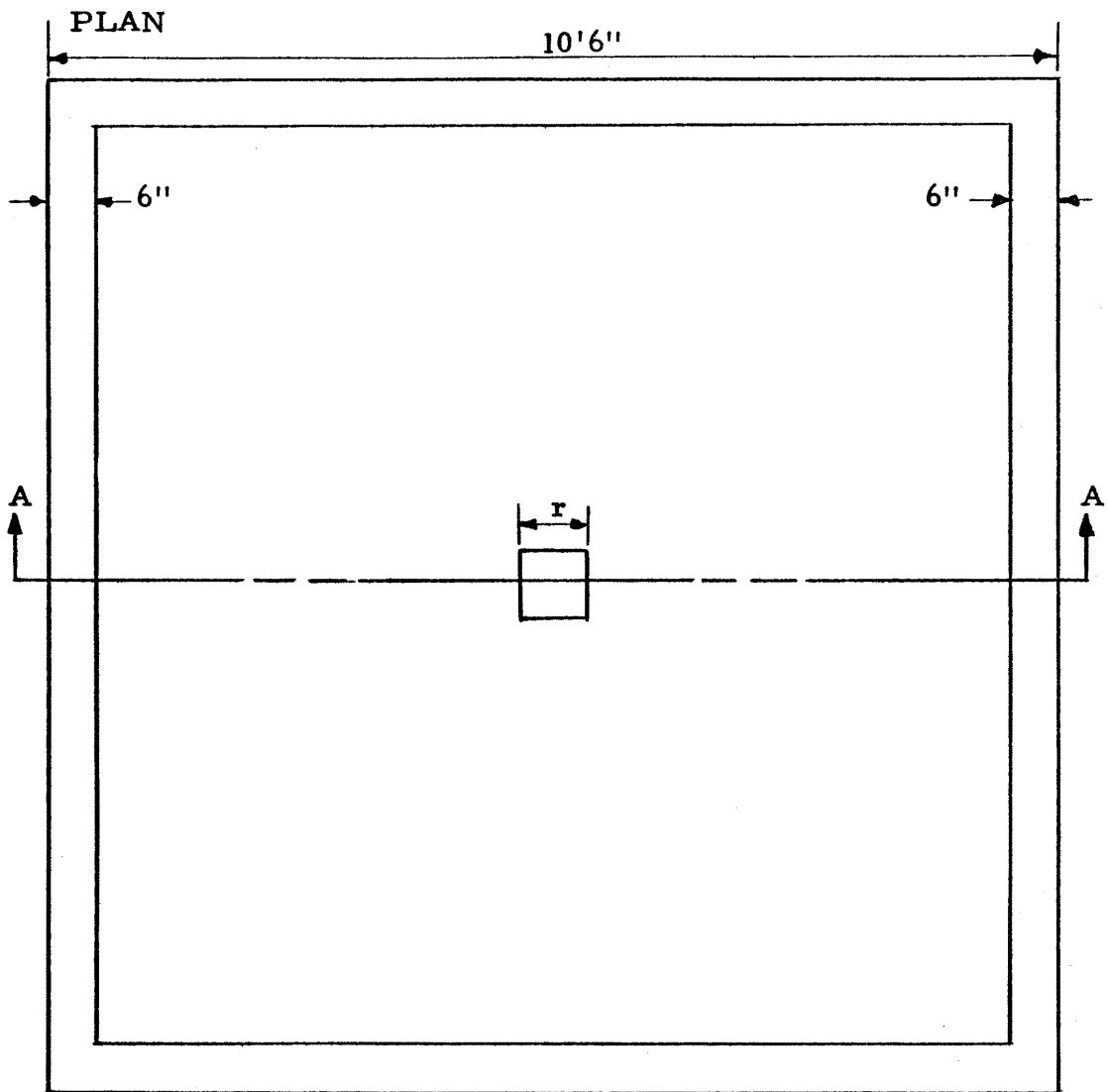
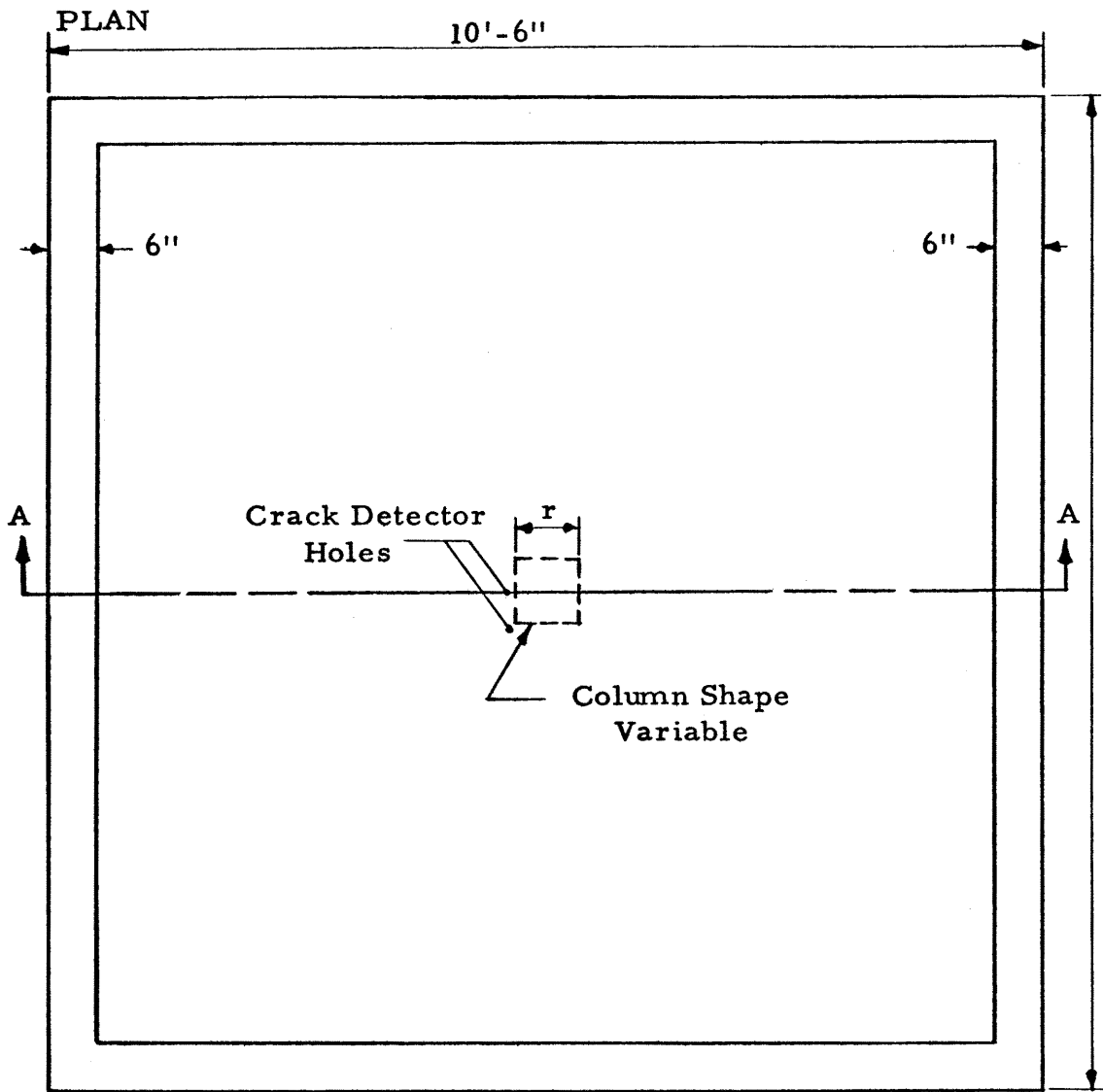


Fig. 2. 2. Proposed Specimen



SECTION A-A

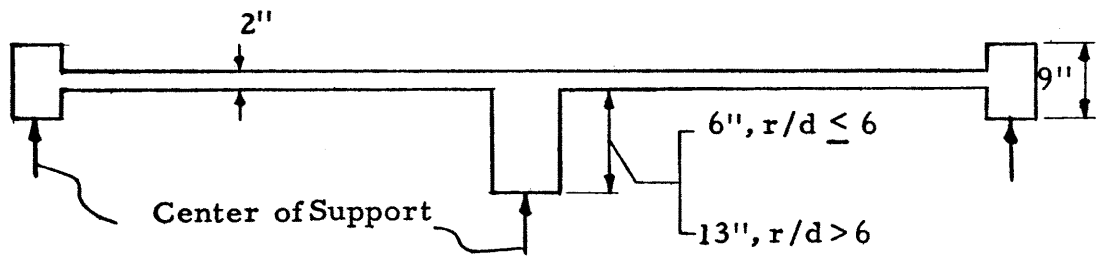


Fig. 2.3. Test Specimens

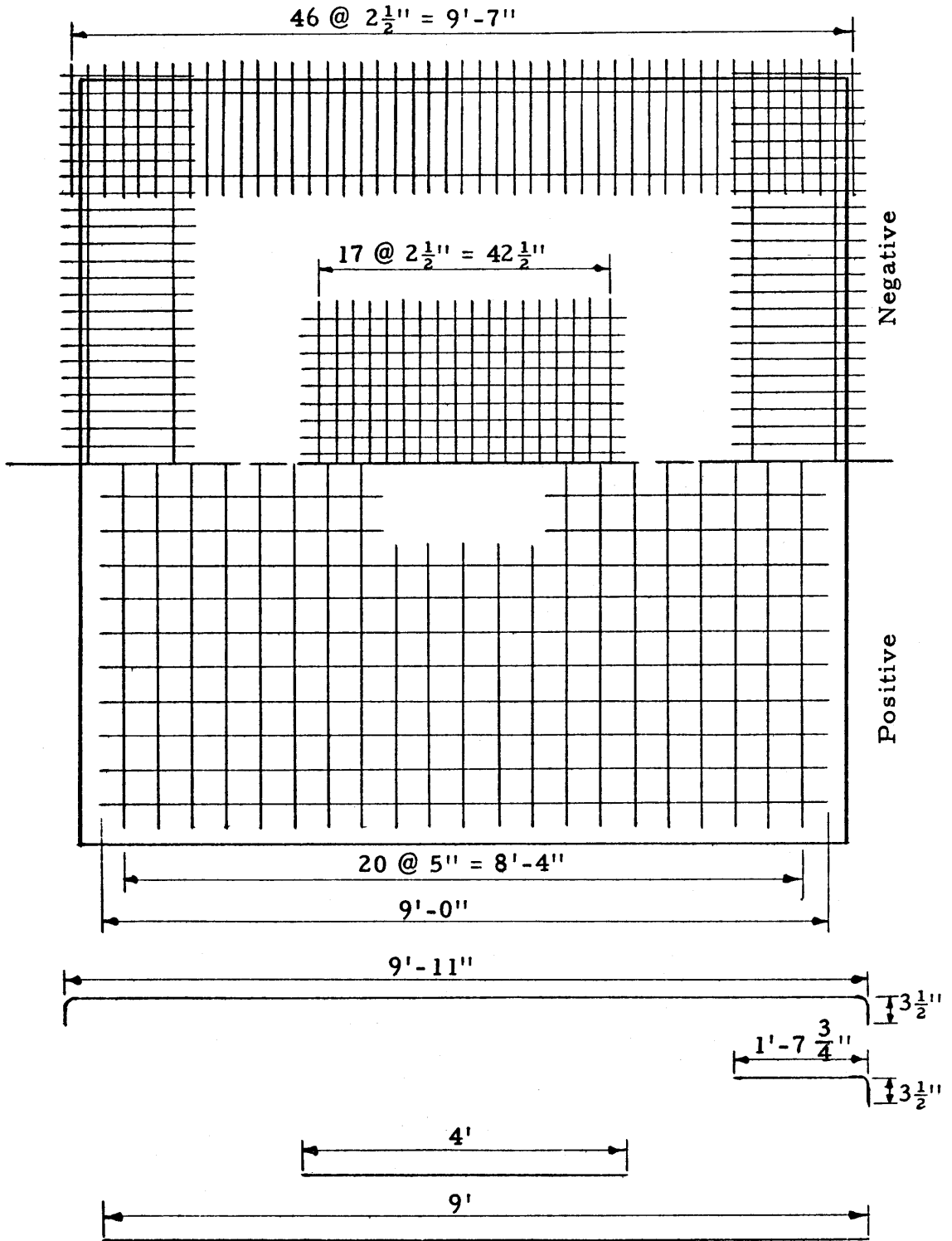


Fig. 2.4. Steel Layout, 1% Negative

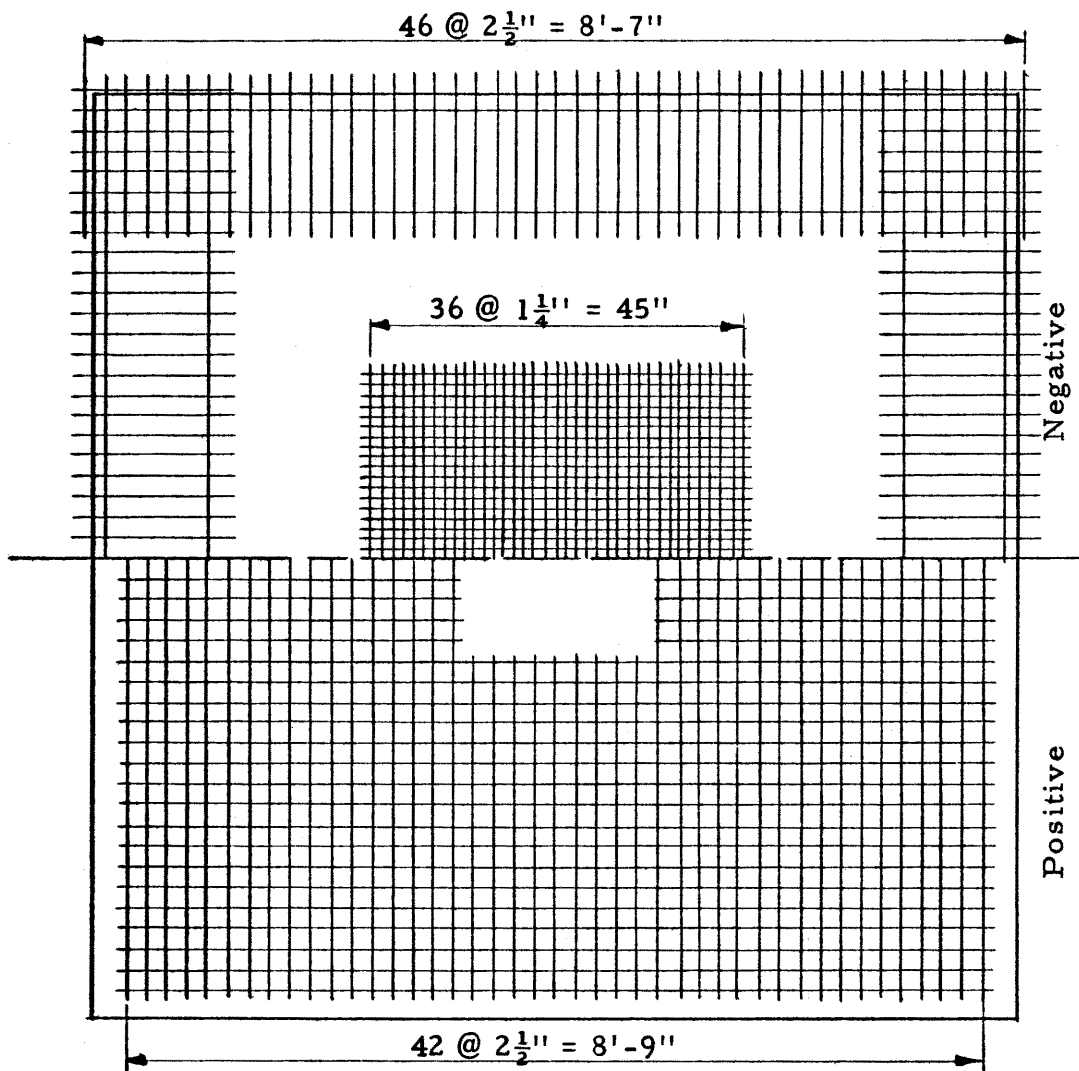
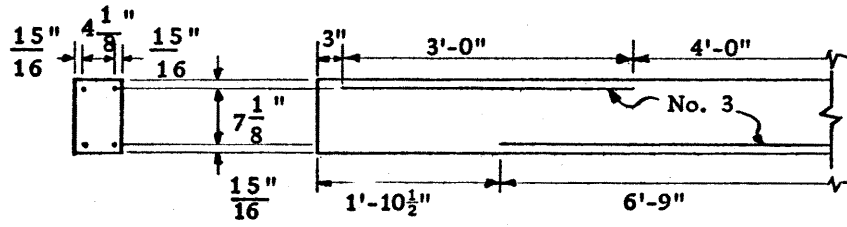
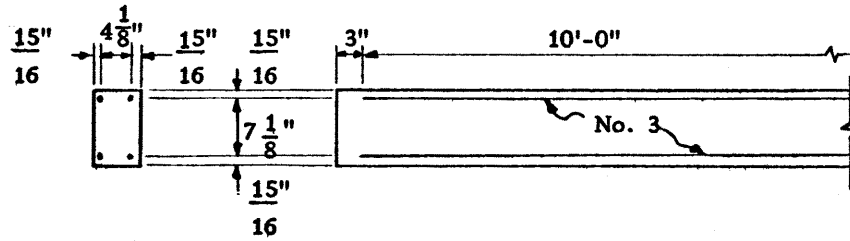


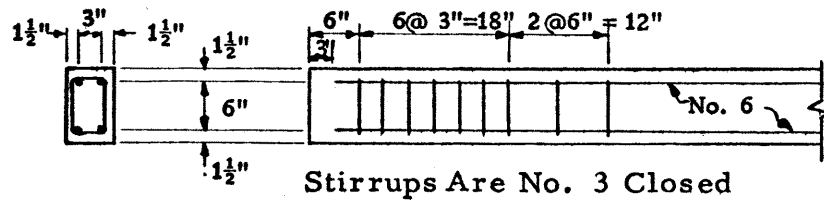
Fig. 2.5. Steel Layout, 2% Negative



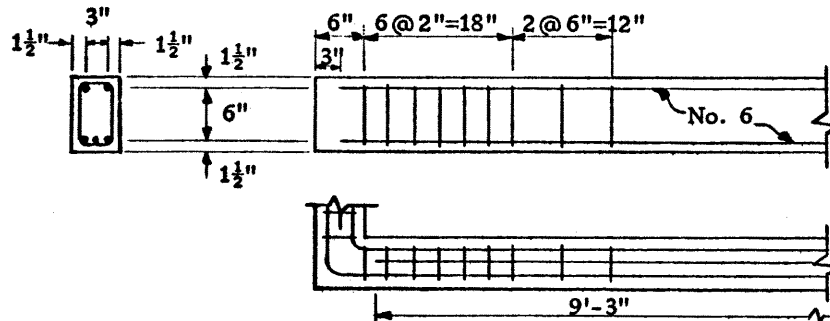
a.



b.



c.



d.

Fig. 2.6. Beam Steel

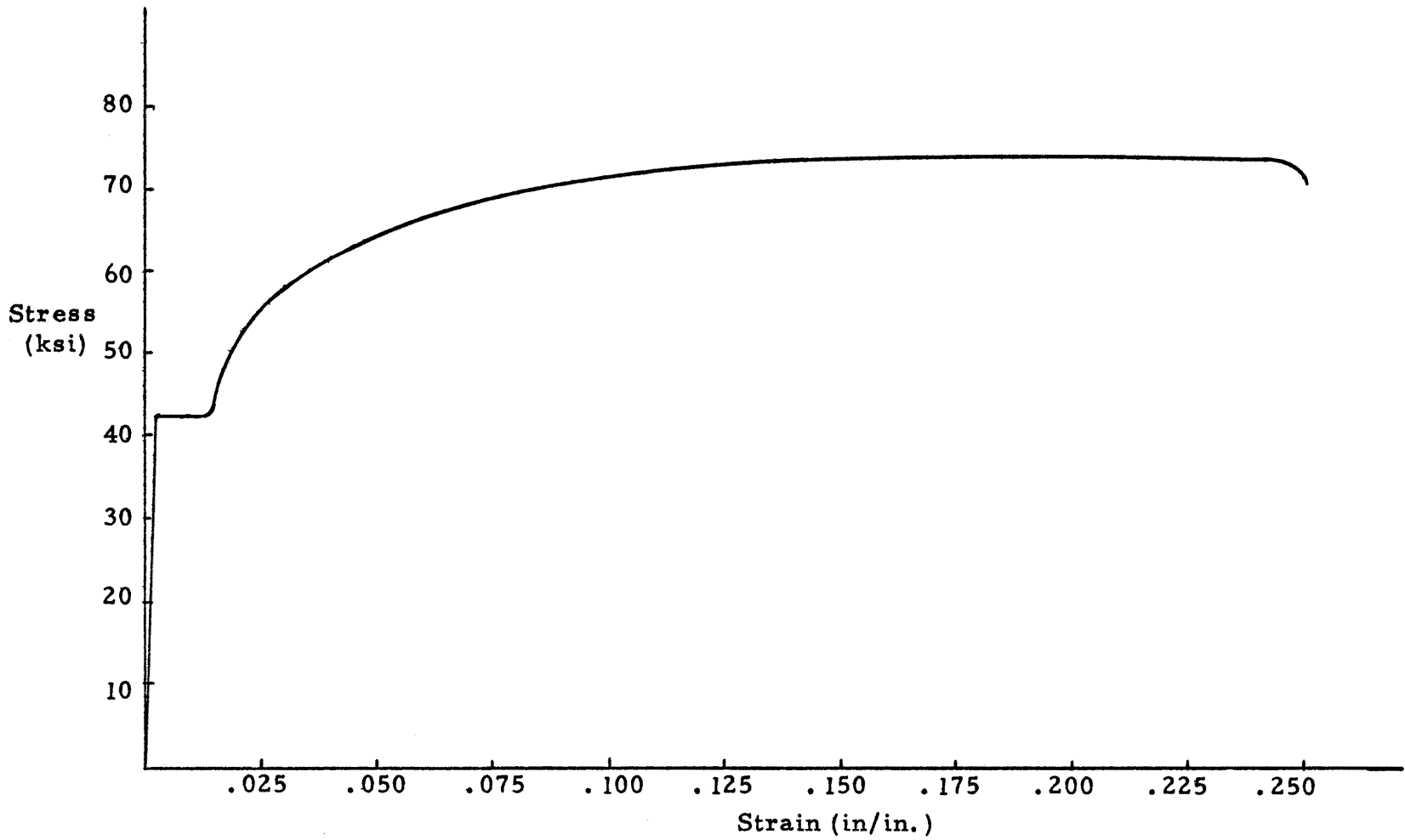


Fig. 2.7. Typical Stress-Strain Curve, Batch No. 1

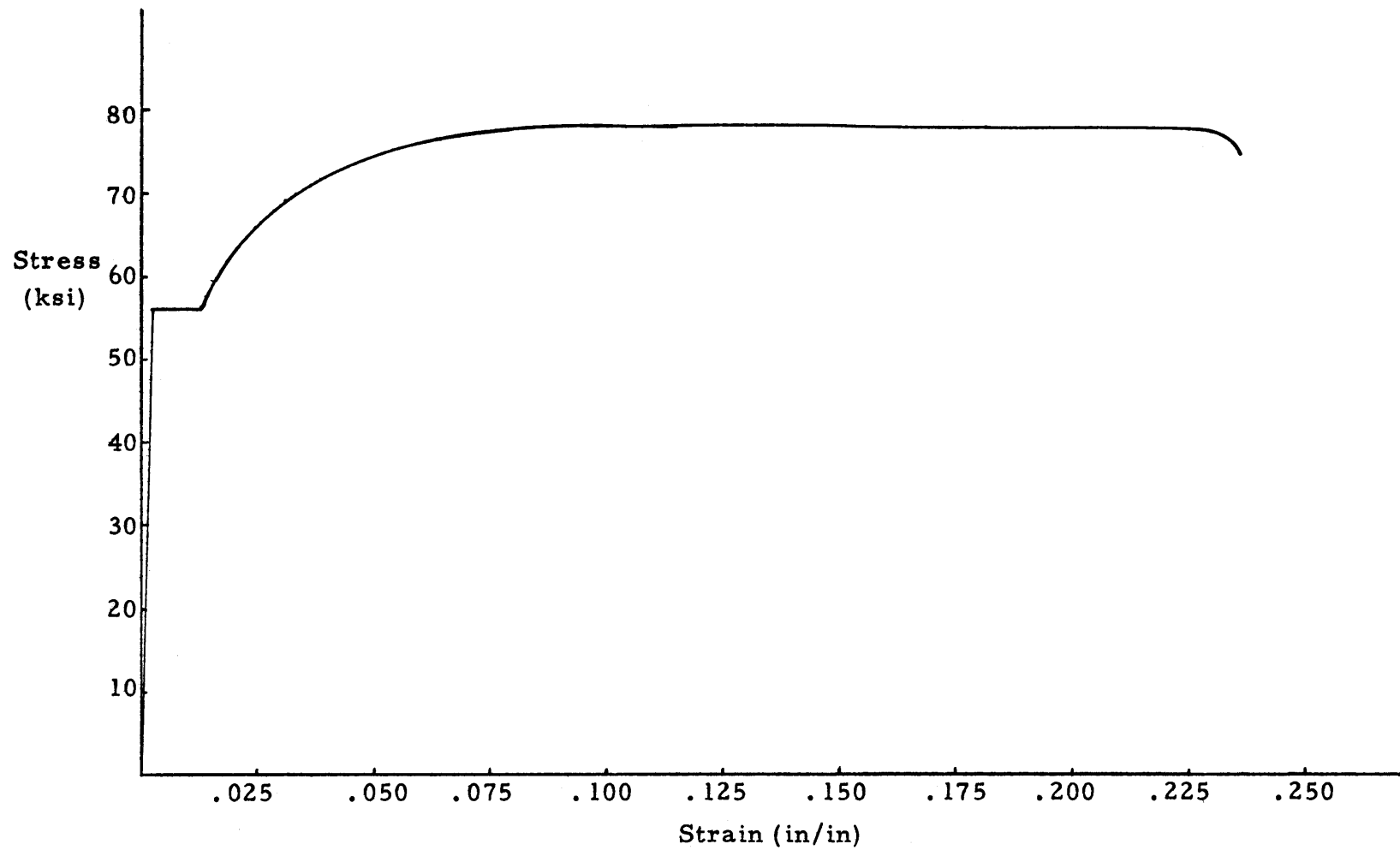
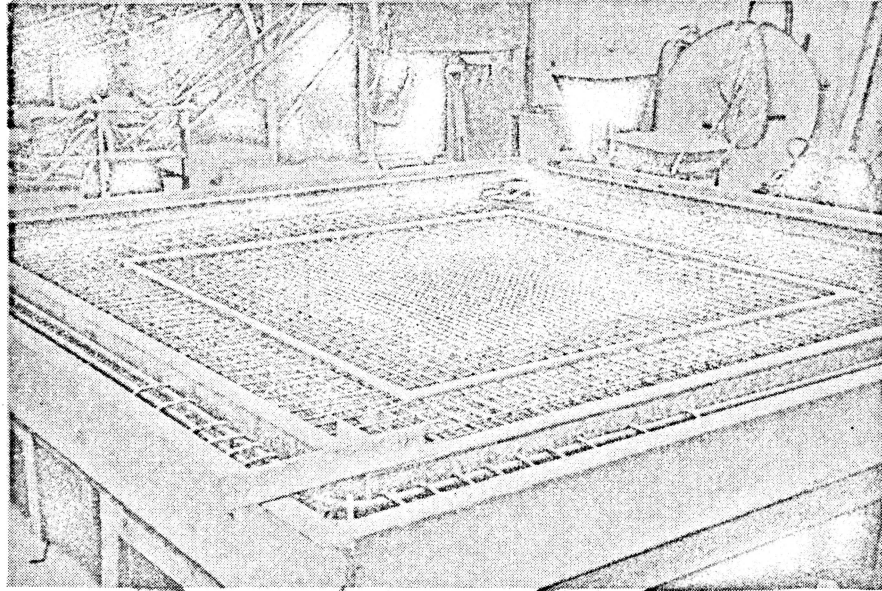
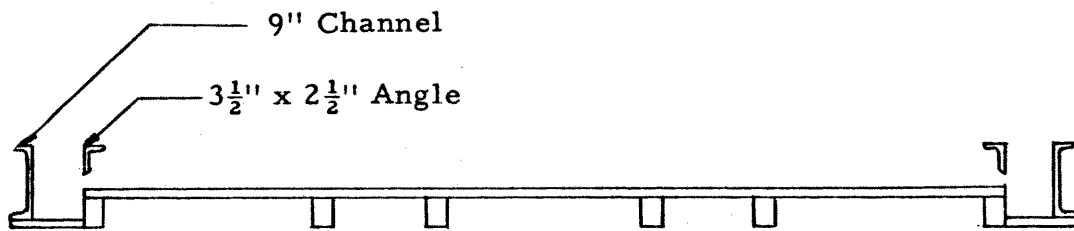


Fig. 2.8. Typical Stress Strain Curve, Batch No. 2



a. Form with 2% Negative Steel in Place



b. Section Through Form

Fig. 2.9. Formwork for Specimen

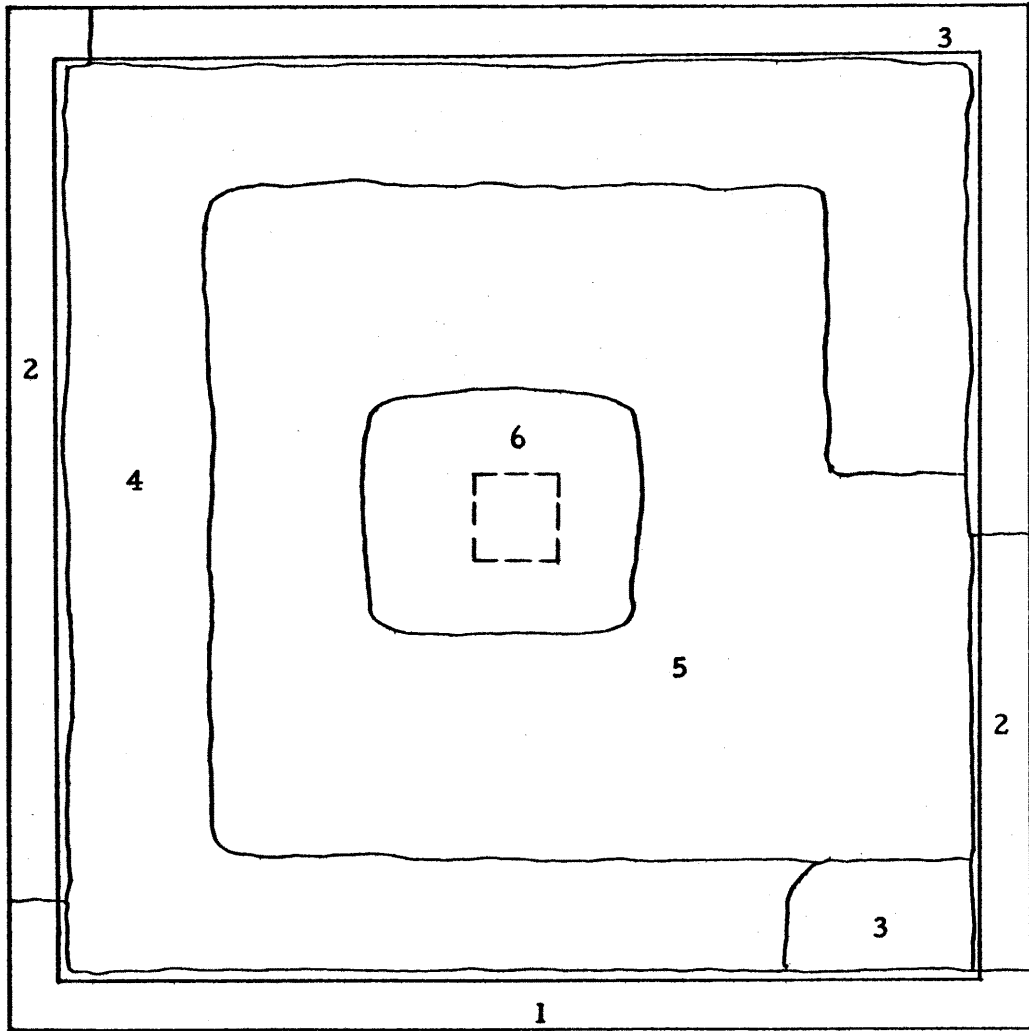


Fig. 2. 10. Approximate Batch Locations

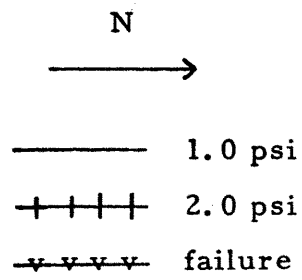
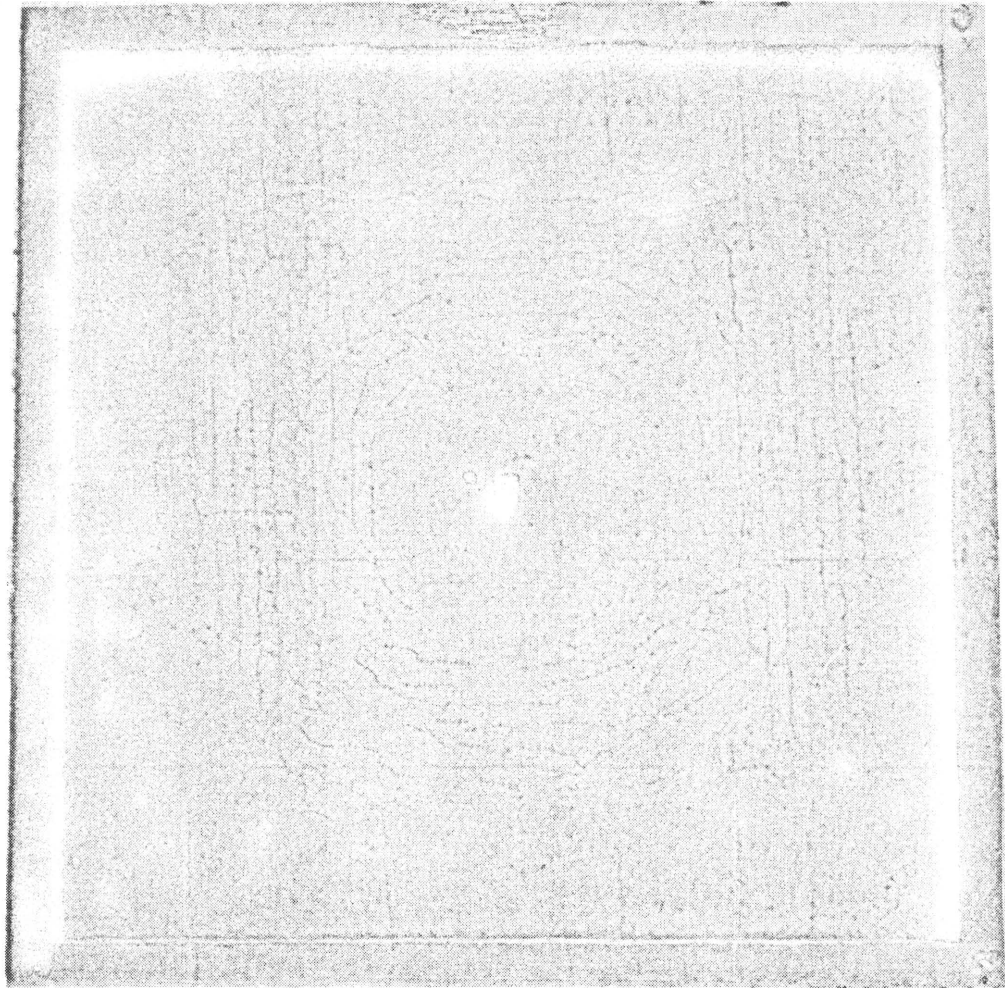


Fig. 3.1. Crack Pattern, Specimen 2S2-7

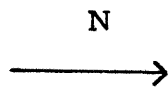
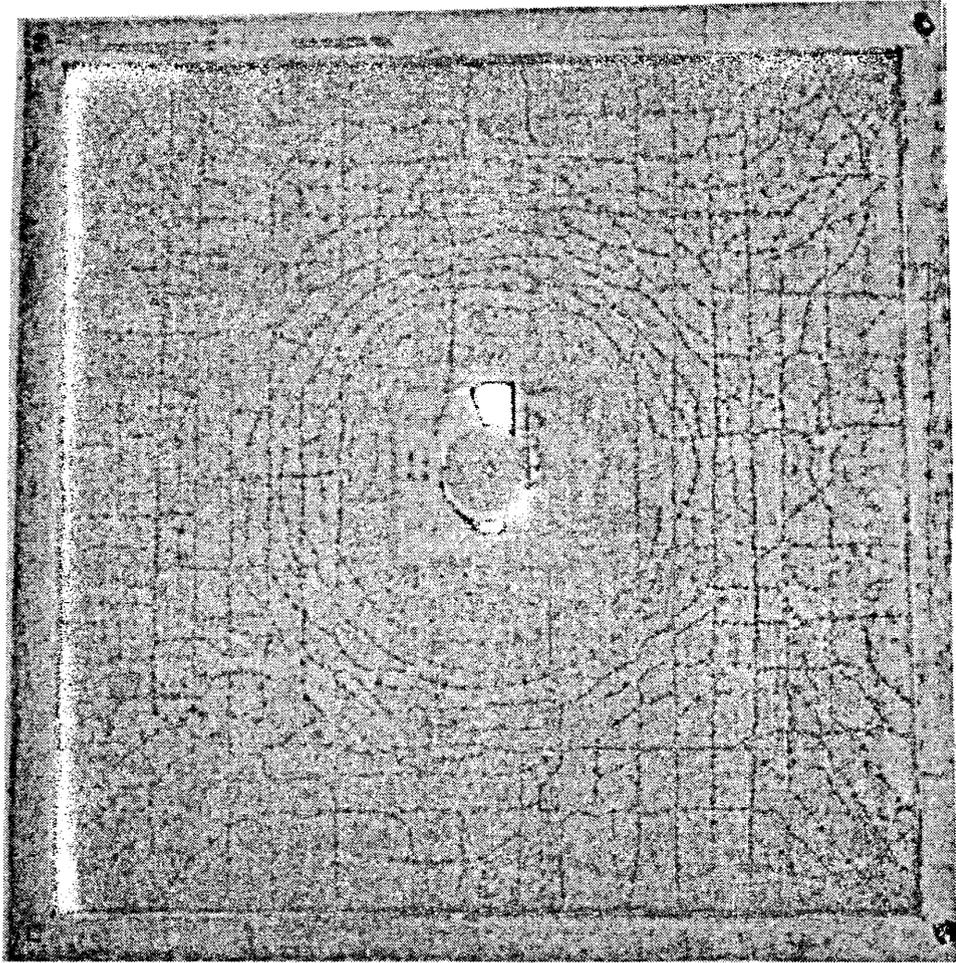


Fig. 3.2. Crack Pattern, Specimen 6Cl-9

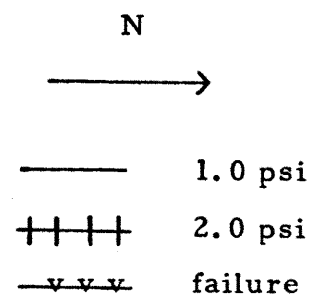
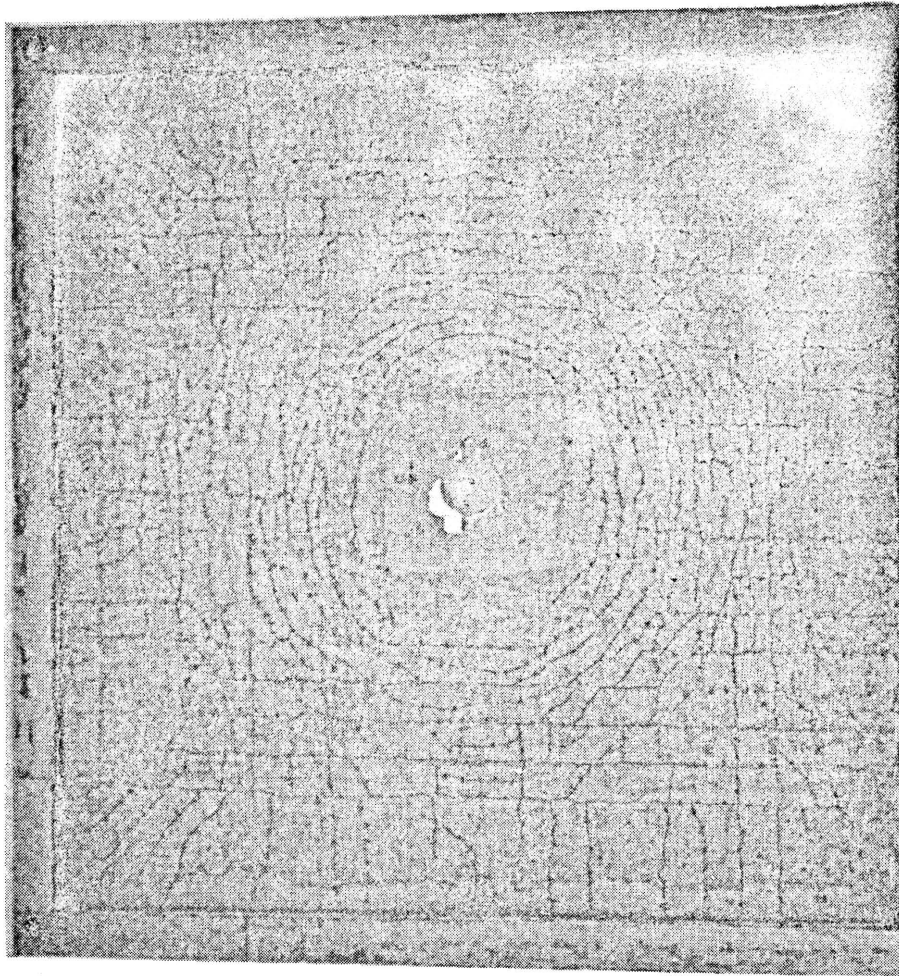


Fig. 3.3. Crack Pattern, Specimen 4C1-12

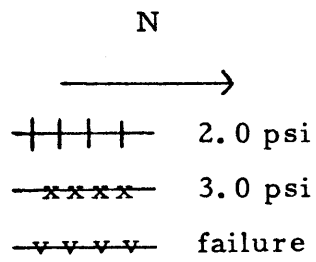
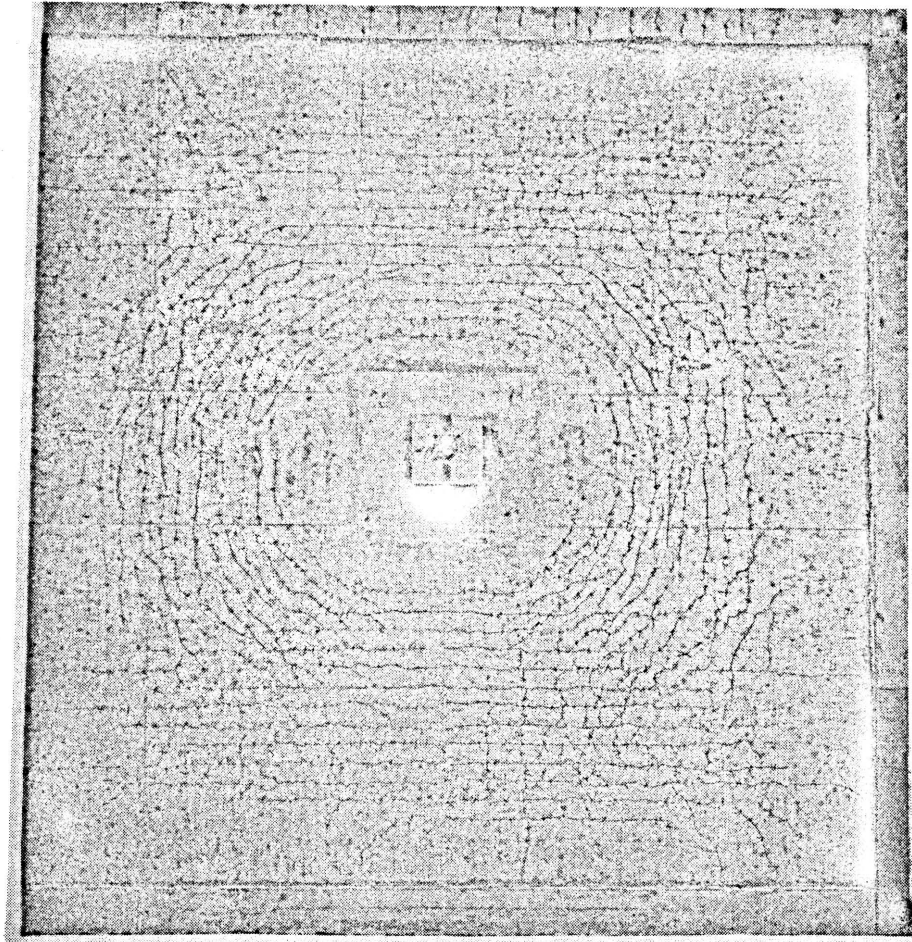


Fig. 3.4. Crack Pattern, Specimen 6S2-14

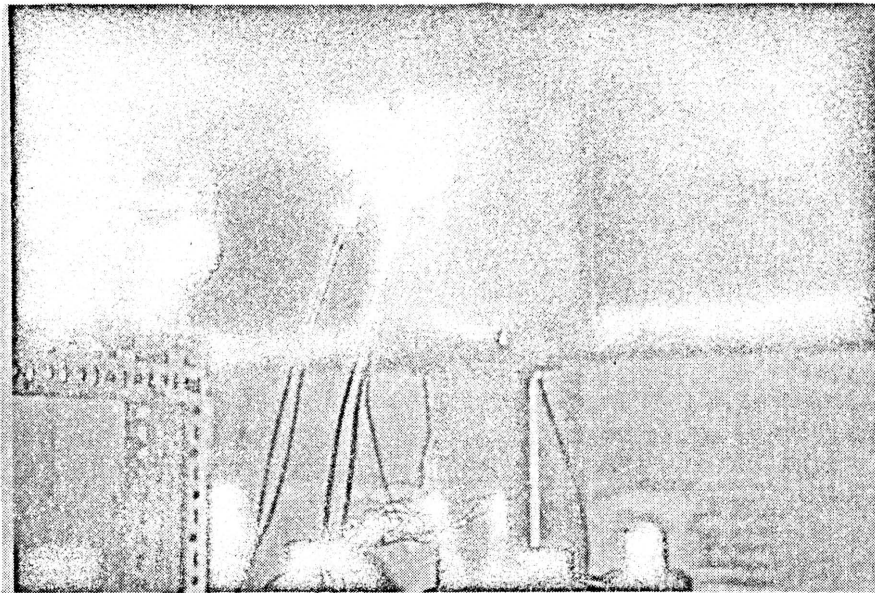


Fig. 3.5. Crack Detectors in Place

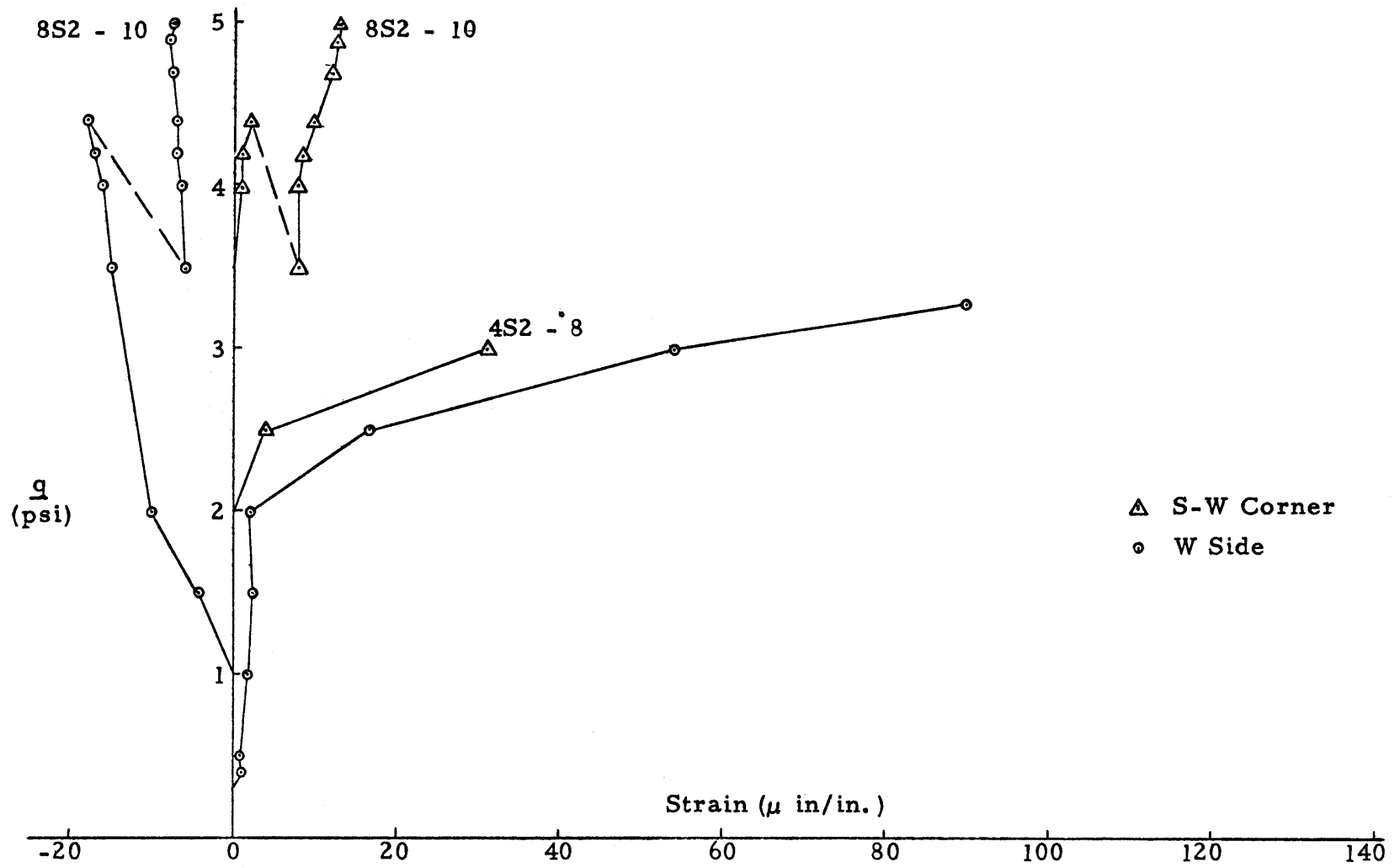


Fig. 3.6. Load vs. Strain in Crack Detector Gages

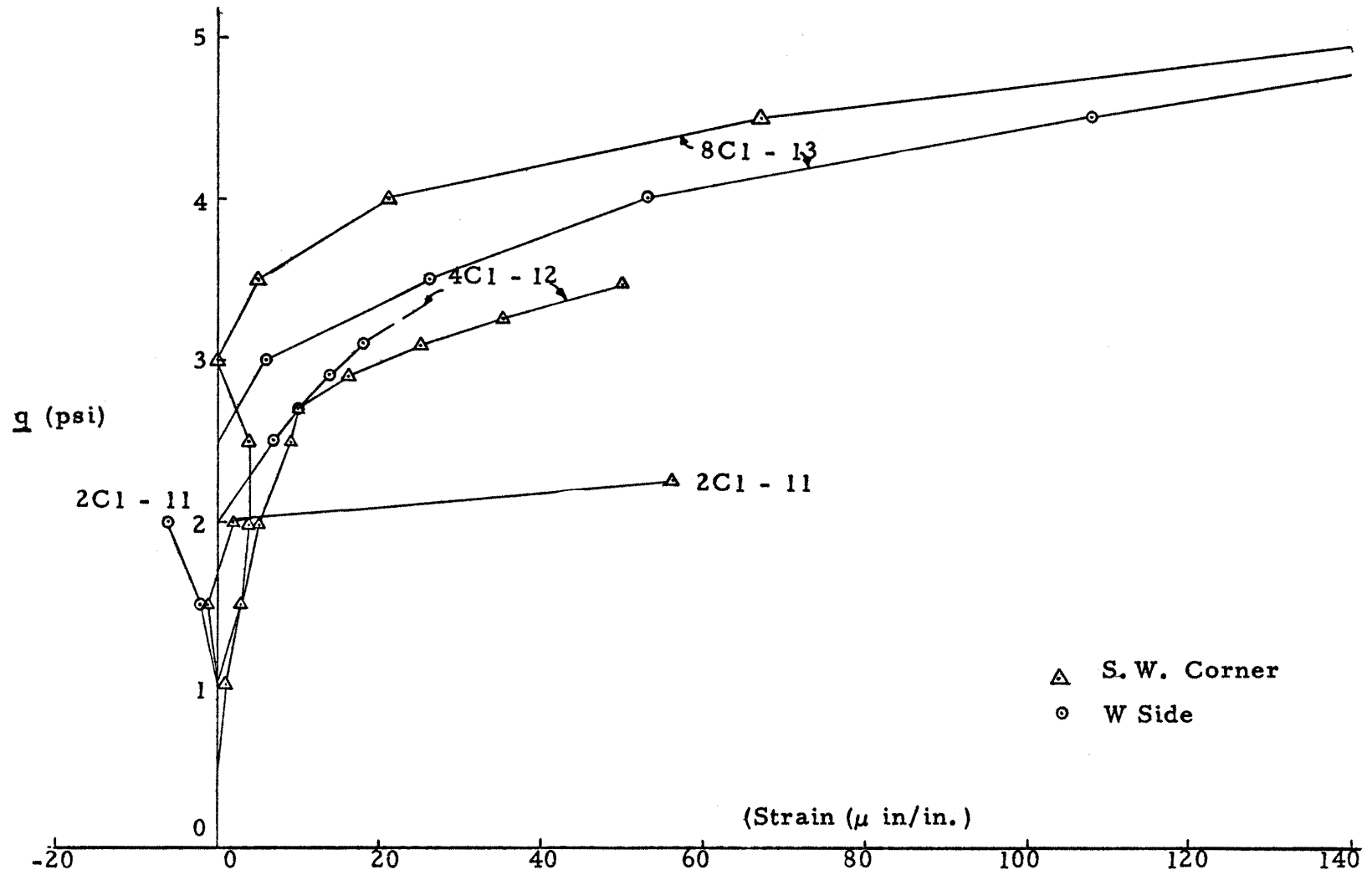


Fig. 3.7. Load vs. Strain in Crack Detector Gages

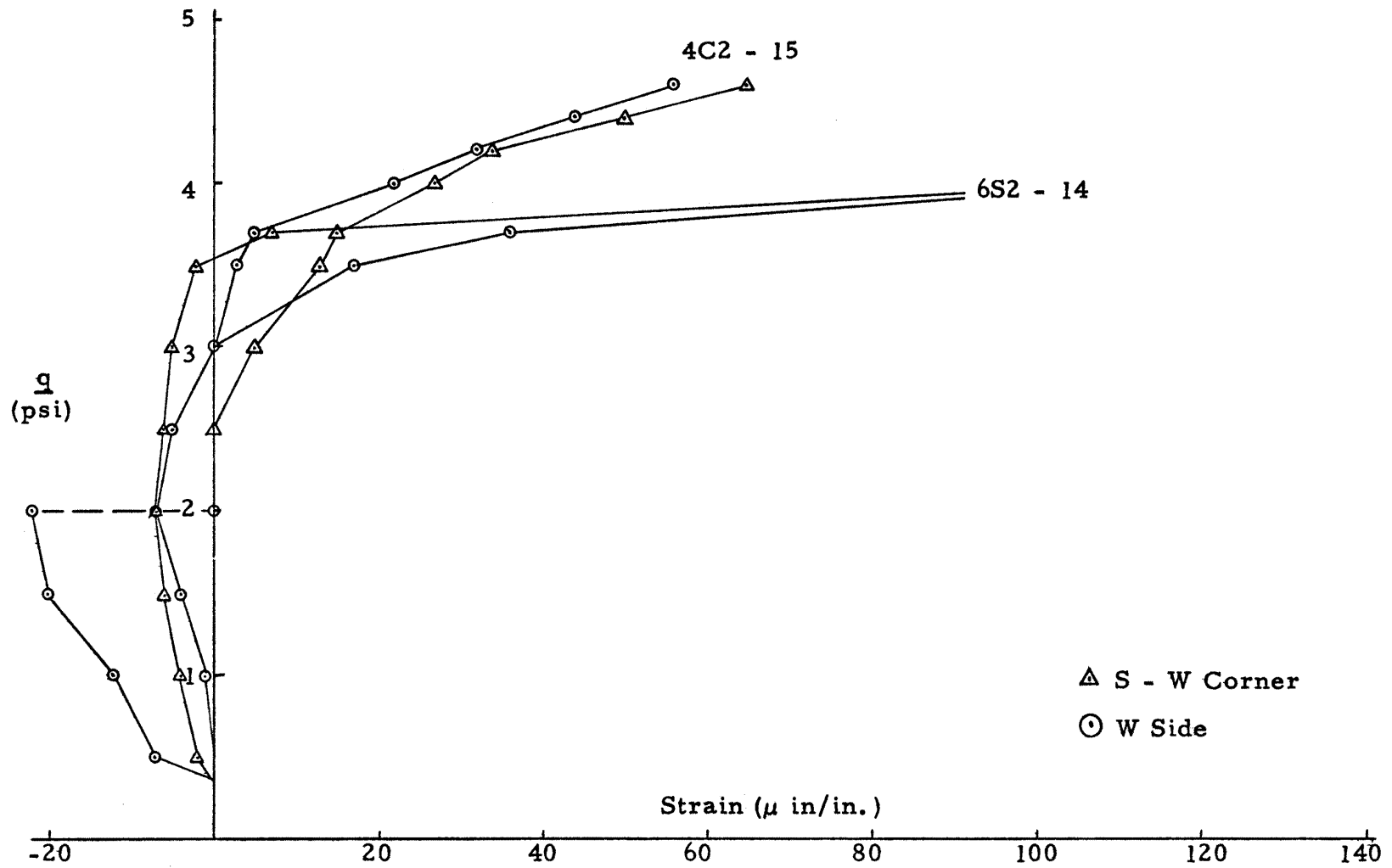
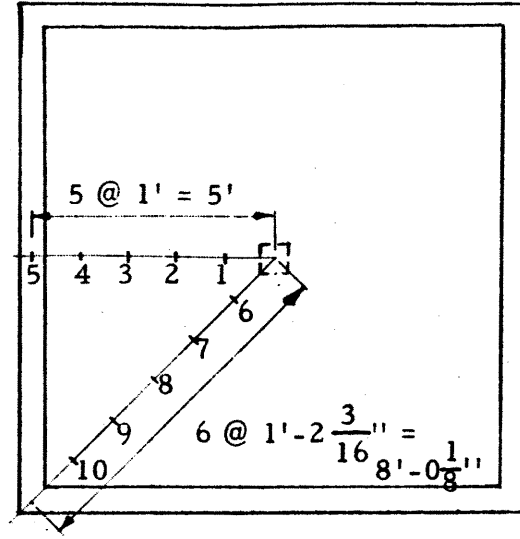
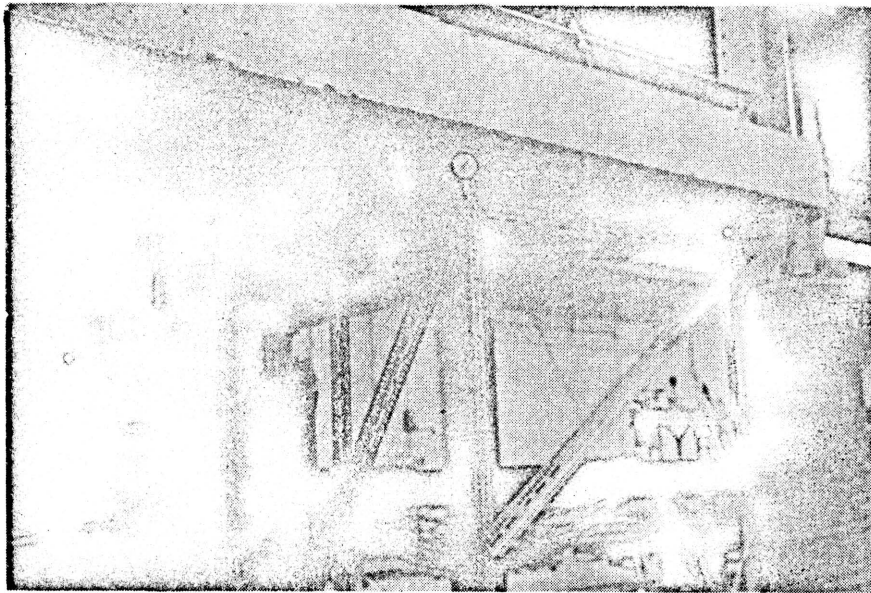


Fig. 3.8. Load vs. Strain in Crack Detector Gages



a. Gage Location



b. Gages in Place

Fig. 3.9. Dial Gage Location and Setup

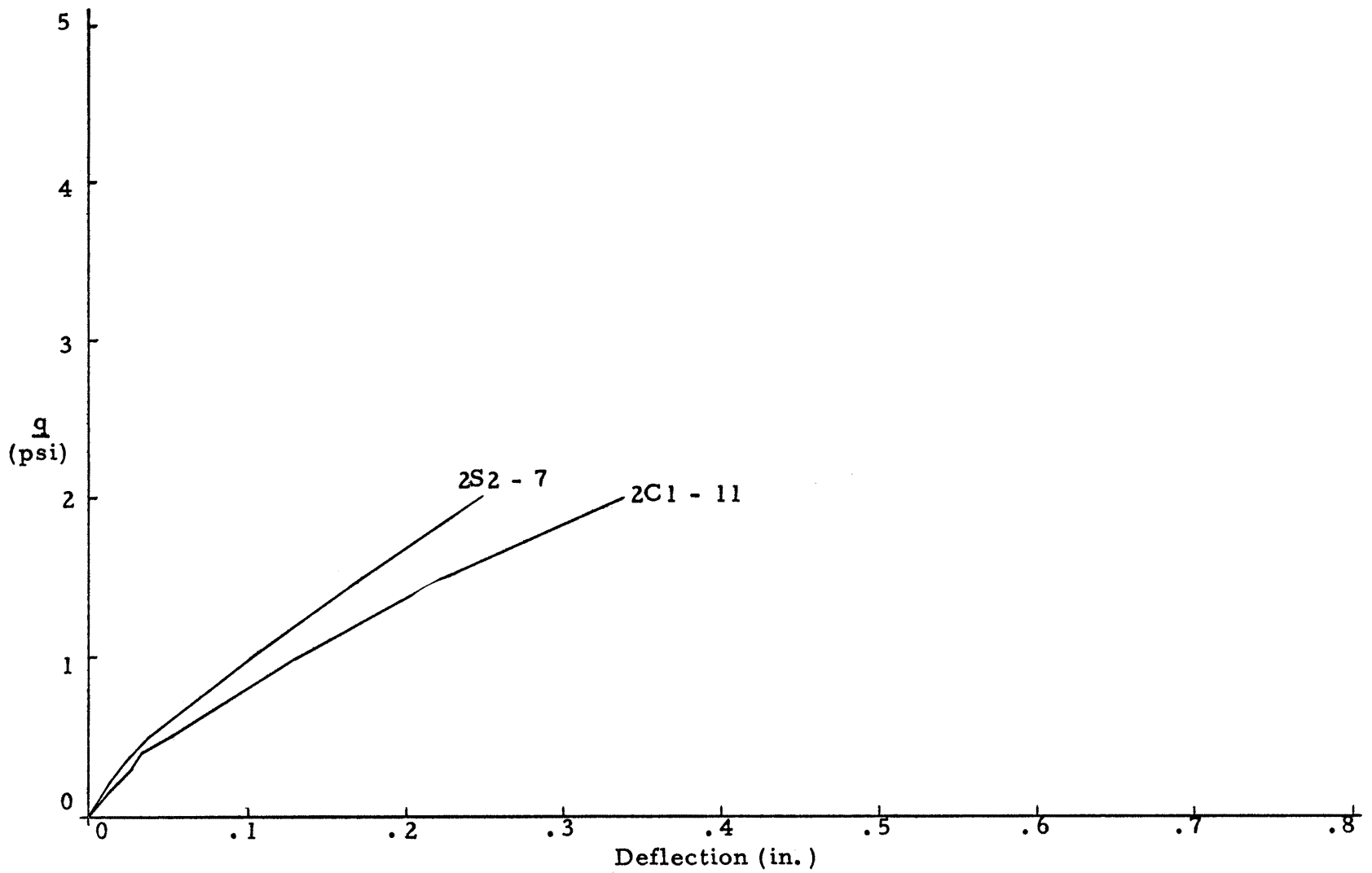


Fig. 3.10. Load vs. Deflection, $r/d = 2$

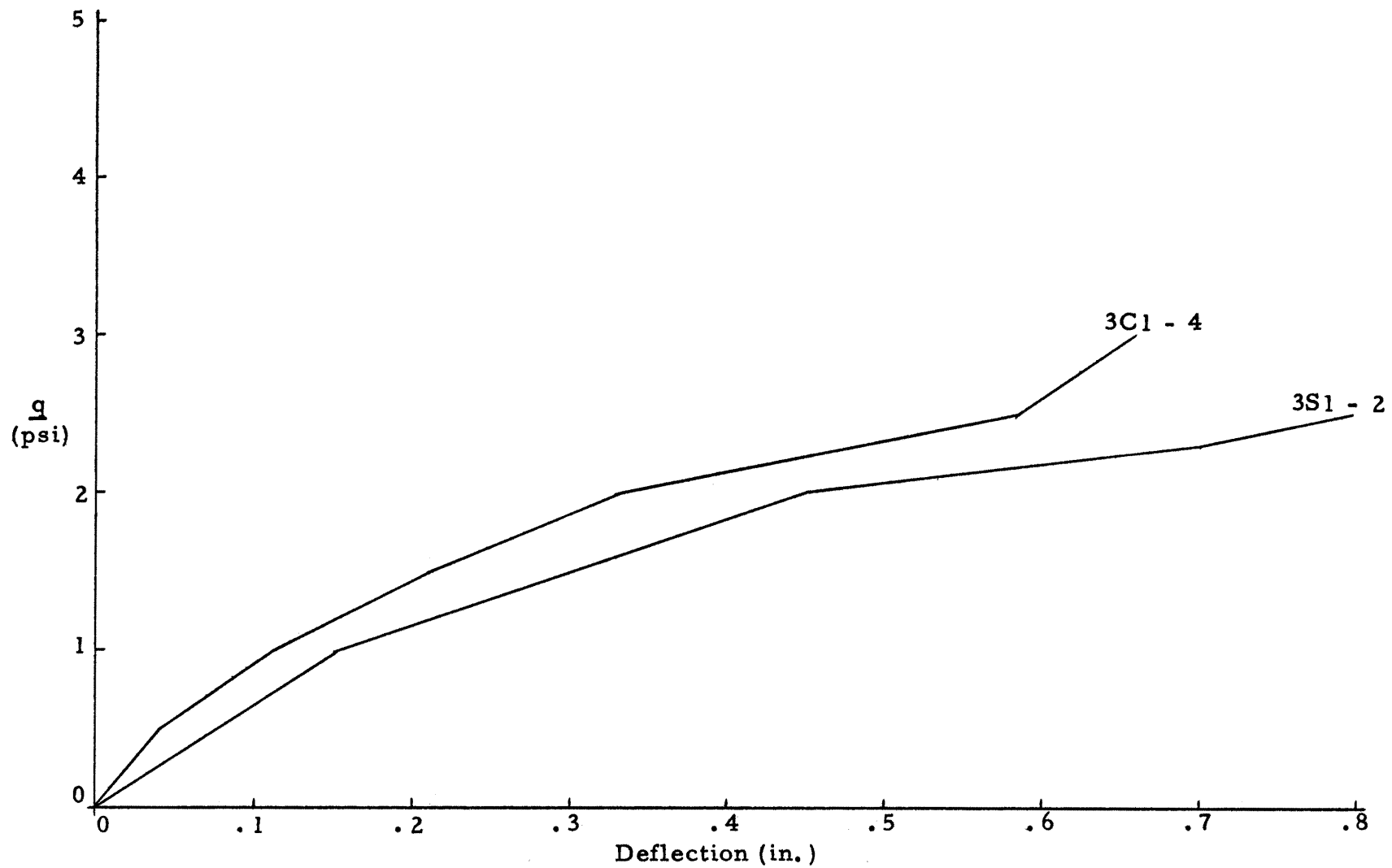


Fig. 3.11. Load vs. Deflection, $r/d = 3$

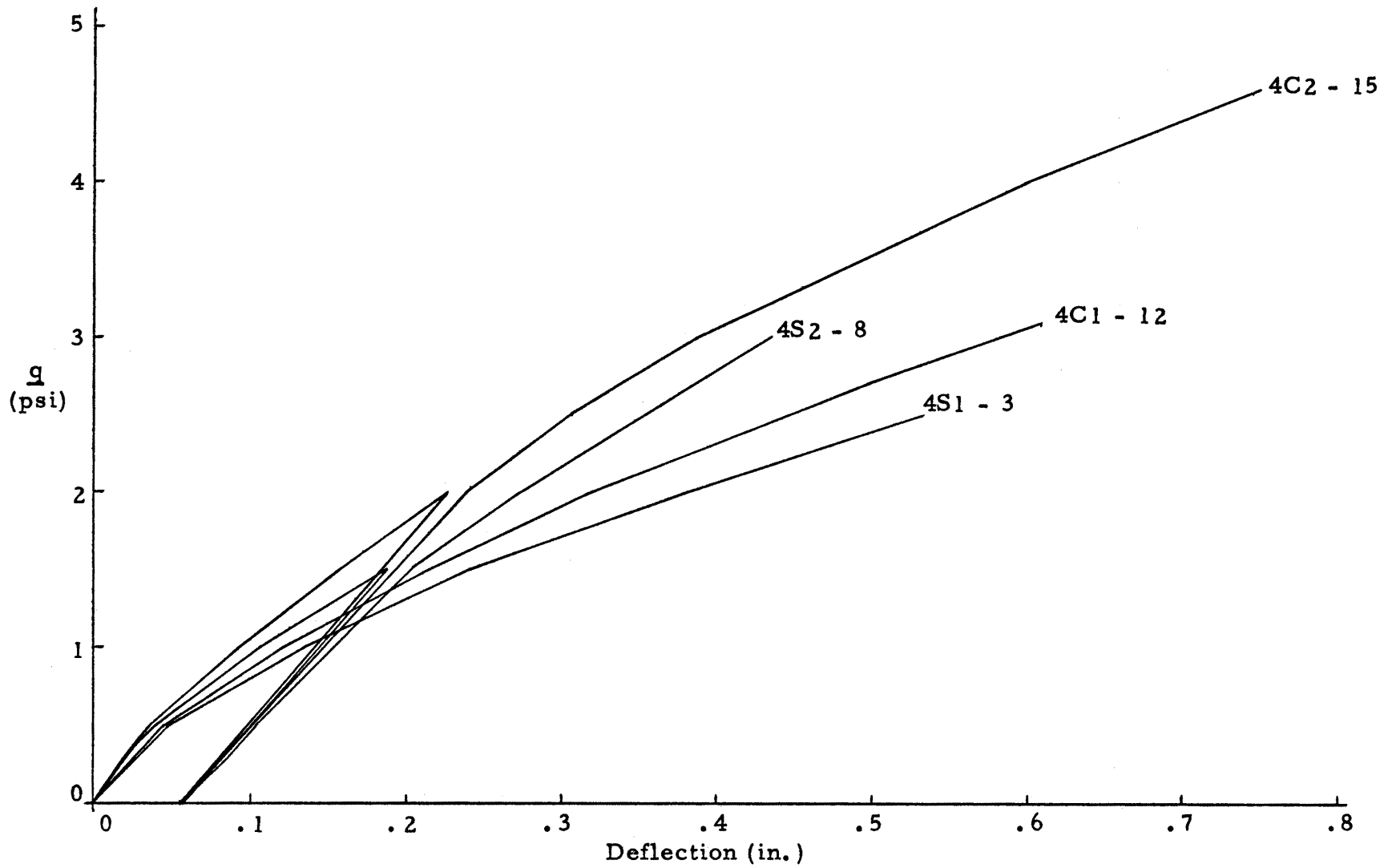


Fig. 3.12. Load in Deflection, $r/d = 4$

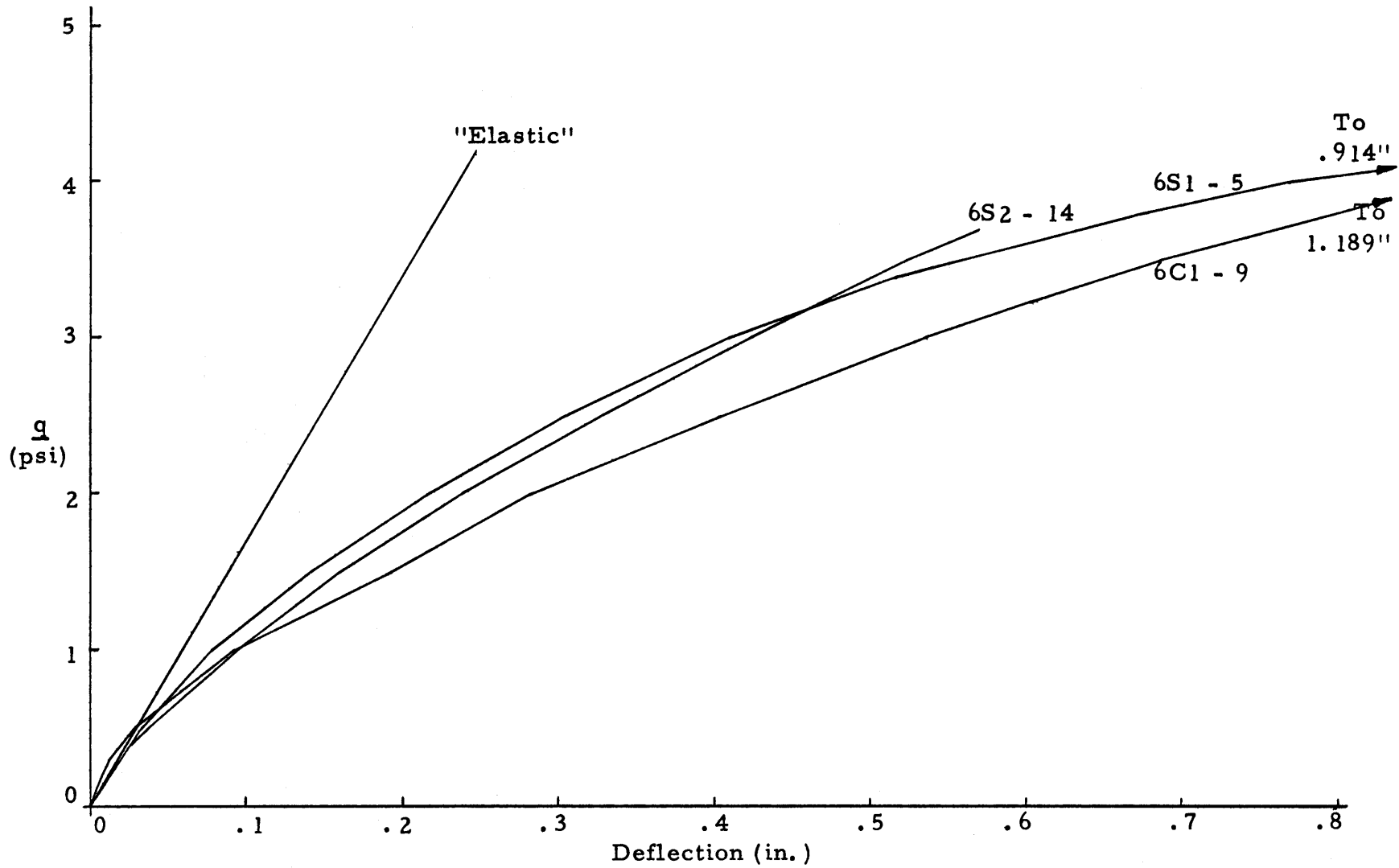


Fig. 3.13. Load vs Deflection, $r/d = 6$

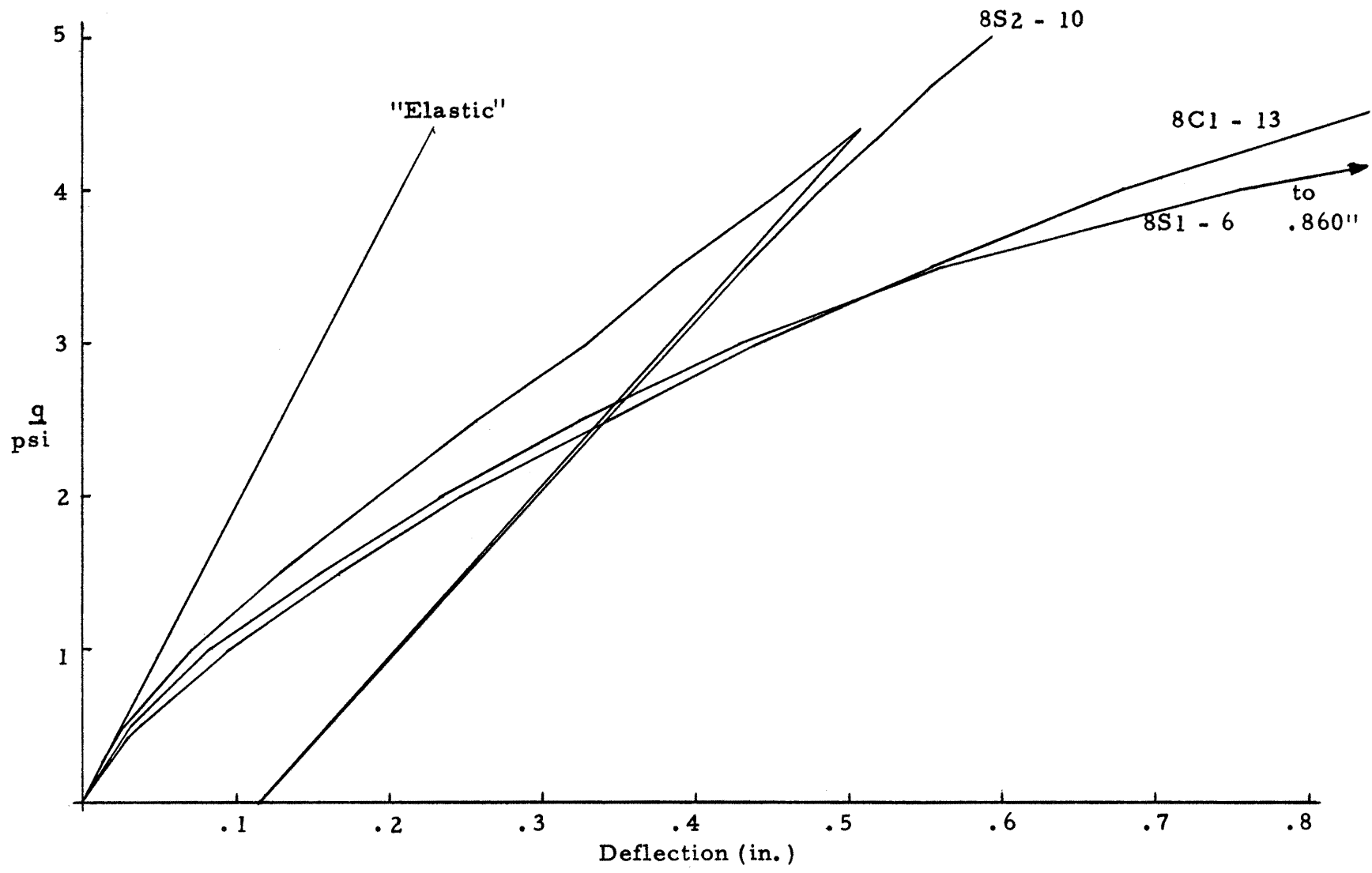


Fig. 3.14. Load vs. Deflection, $r/d = 8$

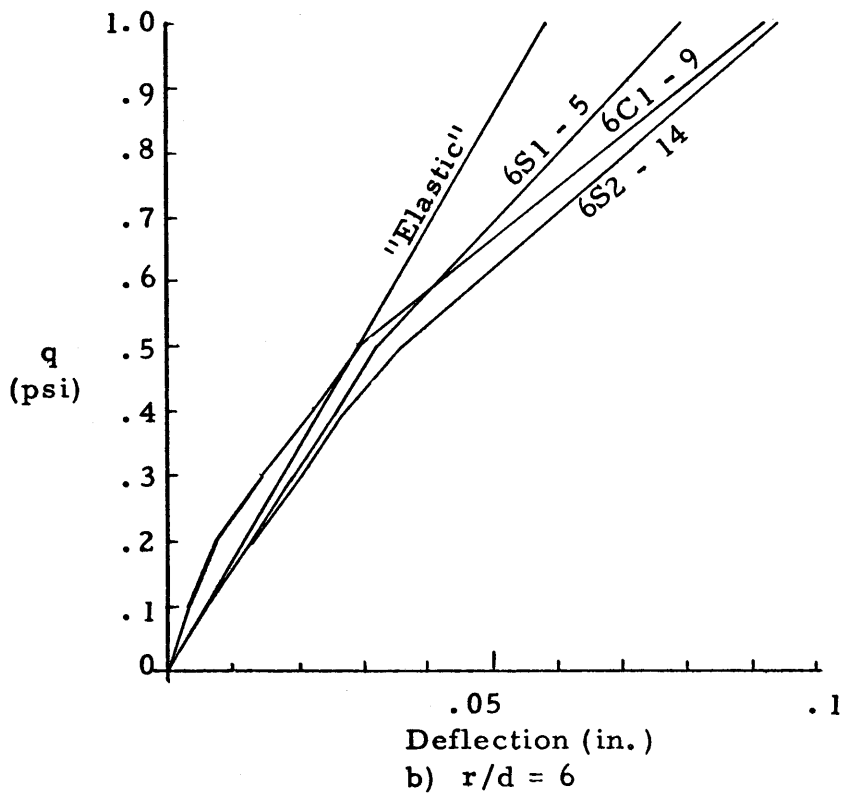
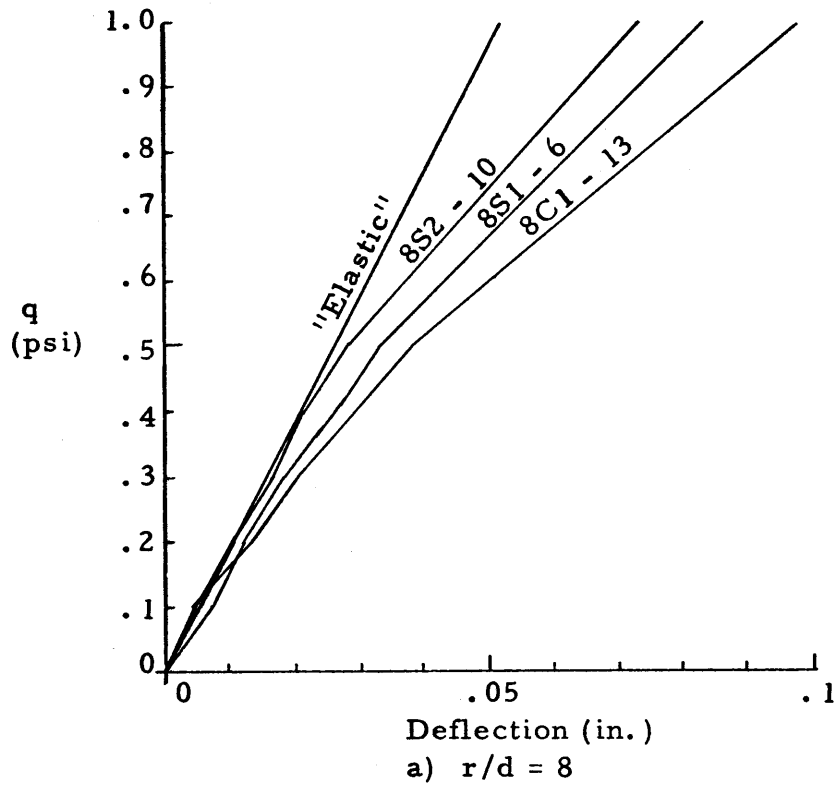


Fig. 3.15. Comparison of Elastic Analysis and Test Specimens, Load vs. Deflection

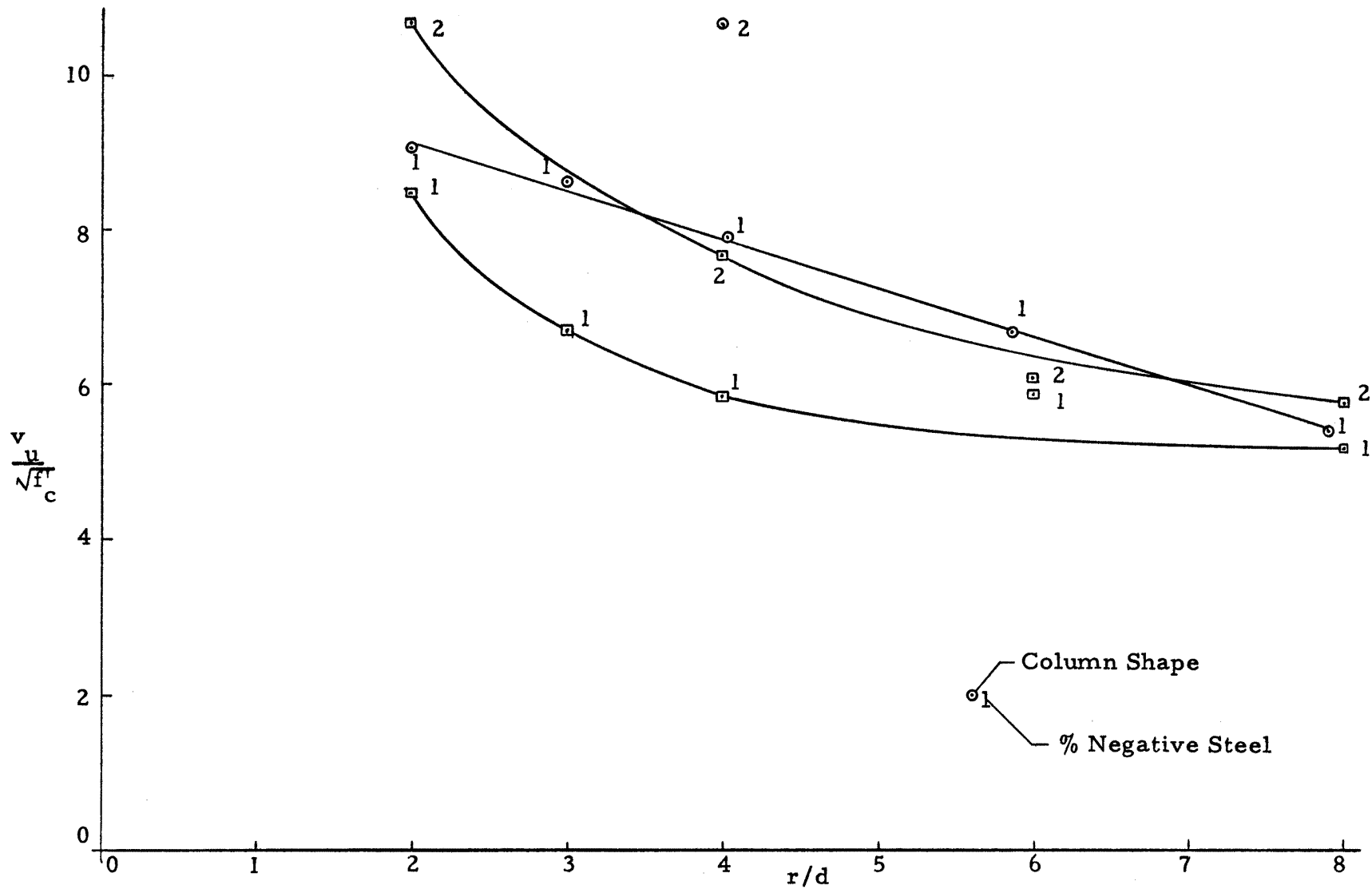


Fig. 3.16. $v_u/\sqrt{f_c}$ vs. r/d

APPENDIX

APPENDIX A

FLEXURAL STRENGTH ANALYSIS

A.1 Introductory Remarks

A yield-line analysis was performed on a mathematical model of the test specimen, to determine the flexural collapse load for use in the various shear strength equations.

The yield-line pattern used was a modified version of one found in Jones and Wood (13) which had simply supported edges, and a point column at the center. This pattern was modified to include clamped edges and a finite rectangular column. Since the negative moment capacity of the test specimen at the center was different from that at the edge, and both were different from the positive moment capacity, this modification was also necessary.

A study showed that the addition of corner levers to the Jones and Wood solution had the effect of lowering the flexural load by only 4 or 5%. For simplicity, it was decided to eliminate consideration of corner levers from the clamped edge, finite column analysis, and to reduce the resulting collapse load by 5%.

Section A. 2 describes the pattern used, and the resulting work equations. Section A. 3 sets forth the results. Section A. 4 describes the method used to calculate V_{flex} from the flexural capacities.

Notation used only in Appendix A is given below.

i = ratio of interior negative moment capacity to positive moment capacity.

j = ratio of exterior negative moment capacity to positive moment capacity.

L = length of square slab in Fig. A. 1a, or distance from center of column to edge of slab in Fig. A. 2.

m = positive moment capacity of slab per unit width.

M_1 = total moment vector along line shown in Fig. A. 1b.

M_2 = total moment vector along line shown in Fig. A. 1b.

$Q = q/2m$.

q = uniformly distributed load on slab.

r_1 = half width of column on long side.

r_2 = half width of column on short side.

W_e = work done by external loads moving through virtual displacements.

W_i = work absorbed by internal moments along yield lines moving through virtual rotations.

α = ratio of distance from column face to positive yield-line over distance from column face to edge of slab in N-S direction.

β = ratio of distance from column face to edge of interior negative steel over distance from column face to edge of slab in N-S direction.

γ = ratio of distance from column face to positive yield line over distance from column face to edge of slab in E-W direction.

δ = unit virtual displacement.

ϵ = ratio of distance from column face to edge of interior negative steel over distance from column face to edge of slab in E-W direction.

θ = rotation vector along yield-line.

λ = angle between moment and rotation vectors in Fig. A. 1c.

ϕ = angle shown in Fig. A. 2.

ω = angle shown in Fig. A. 2.

A. 2. Analysis

The method of virtual work was used in the analysis. The virtual work procedure is based on the condition that the work done due to the application of a virtual displacement to a system in equilibrium must be zero (8). Mathematically this may be expressed as

$$\Sigma W_e + \Sigma W_i = 0 \quad (A1)$$

where ΣW_e is the total work done by external loads moving through virtual translations, and ΣW_i is the total work absorbed by internal moments along yield lines moving through virtual rotations. Since the virtual work expression is often misstated in the literature (3) or awkward schemes are evolved for computational use (13) a simple example is described in detail below to show the correct procedure.

Consider a square, simply supported slab as shown in Fig.

A. 1a. The slab carried a uniform unit load, q , moment capacities

in orthogonal directions are the same, and corner levers are ignored. One quadrant of the slab is shown as a free body in Fig. A. 1b.

Since external work is defined as load times displacement the W_e term is found as

$$W_e = \int_0^{L/2} dW_e = \int_0^{L/2} q(L - 2x)(dx) \frac{(\delta x)}{0.5L} = \frac{qL^2}{12} \delta. \quad (A2)$$

The moment and rotation vectors for the quadrant shown in Fig. A. 1b are found using the right hand rule for vectors. Since the rotation and moment vectors are not colinear it is necessary to compute internal work using the dot product definition of vector multiplication, which applies also to the external work term. The work done by the moment M_2 is found by laying out the M_2 and θ vectors tail-to-tail as shown in Fig. A. 1c, and is computed as

$$W_i = \theta \cdot M_2 = |\theta| \times |M_2| \times \cos \lambda \quad (A3)$$

or

$$W_i = \frac{\delta}{0.5L} \times \frac{mL}{\sqrt{2}} \cos 135^\circ = -\delta m \quad (A4)$$

Since $|M_1| = |M_2|$ the total internal work is

$$W_i = -2\delta m \quad .$$

For the entire structure Equation A1 is

$$\frac{4q(L^2 \delta)}{12} - \delta 8m = 0$$

or

$$q = \frac{24m}{L^2} \quad (A5)$$

The scheme described above was used in obtaining the following solution.

The yield-line pattern used is shown in Fig. A. 2. The constants ϵ and β represent the distance from the faces of the column to the edge of the center mat of the negative steel. From trigonometry the constants γ and α are shown to be equal

$$\tan \omega = \frac{\gamma(L - r1)}{\alpha(L - r2)} \quad (A6)$$

$$\tan \omega = \frac{(L - r1)}{(L - r2)} \quad (A7)$$

$$\frac{\gamma}{\alpha} = 1 \quad (A8)$$

A preliminary solution using clamped edges, point columns, and keeping the negative steel constant across the slab, showed the effect of corner levers to be about a 5% reduction of strength. The results of this solution are shown in Table A. 1.

It was decided not to use corner levers on the clamped edge, finite column solution, since the resulting equations would be considerably more difficult to solve. Instead, the collapse loads calculated on the basis of Fig. A. 2 were reduced by 5%.

The external work expression for each section of the slab was

$$\left. \begin{aligned} W_{eA} &= q\alpha(L - r2) [r1 + 2/3 \alpha(L - r1)] \\ W_{eB} &= q(L - r2)(1 - \alpha) [L - 2/3(L - r1)(1 - \alpha)] \\ W_{eC} &= q\alpha(L - r1) [r2 + 2/3\alpha(L - r2)] \\ W_{eD} &= q(L - r1)(1 - \alpha) [L - 2/3(L - r2)(1 - \alpha)] \end{aligned} \right\} \quad (A9)$$

The internal work expression for each section of slab was

$$\left. \begin{aligned} W_{iA} &= \frac{-2m}{\alpha} \left[i\beta \cot \phi + \frac{ir1 + \alpha(L - r1) + r1}{(L - r2)} \right] \\ W_{iB} &= -2m \left[\cot \phi + \frac{\alpha(L - r1) + r1 + jL}{(L - r2)(1 - \alpha)} \right] \\ W_{iC} &= \frac{-2m}{\alpha} \left[i\epsilon \cot \omega + \frac{ir2 + \alpha(L - r2) + r2}{(L - r1)} \right] \\ W_{iD} &= -2m \left[\cot \omega + \frac{\alpha(L - r2) + r2 + jL}{(L - r1)(1 - \alpha)} \right] \end{aligned} \right\} \quad (A10)$$

Summing external and internal work, and solving for

$Q = q/2m$ gives:

$$\begin{aligned} Q &= \frac{-1}{\alpha} \left[i\beta \cot \phi + \frac{ir1 + \alpha(L - r1) + r1}{(L - r2)} + i\epsilon \cot \omega + \frac{ir2 + \alpha(L - r2) + r2}{(L - r1)} \right] \\ &\quad - \left[\cot \phi + \frac{\alpha(L - r1) + r1 + jL}{(L - r2)(1 - \alpha)} + \cot \omega + \frac{\alpha(L - r2) + r2 + jL}{(L - r1)(1 - \alpha)} \right] \frac{q}{2} \\ &\quad \alpha \{ (L - r2) [r1 + 2/3\alpha(L - r1)] + (L - r1) [r2 + 2/3\alpha(L - r2)] \} \\ &\quad + (1 - \alpha) \{ (L - r2) [L - 2/3(L - r1)(1 - \alpha)] + (L - r1) \\ &\quad \quad [L - 2/3(L - r2)(1 - \alpha)] \} \quad (A11) \end{aligned}$$

Since the value of α was an unknown variable, the work equation was solved for 100 different values of α for each slab, using a digital computer. The minimum value of Q was selected from these results.

A.3 Results

For each specimen the column size, amount of reinforcement, f'_c , and f_y were input data. From these, the moment capacities were calculated, and hence, the values of q_{flex} were calculated. These values are shown in Table 3.1.

It was also desired to see how Q and α varied with column size. Constant values of i and j were input to the program, and the results plotted graphically. These results are shown in Fig. A.3 and A.4.

A.4 Computation of V_{flex}

The data obtained from the yield-line analysis consisted only of the uniformly distributed load, q_{flex} , corresponding to flexural failure, and the location of the positive yield-line. The determination of the portion of the total load carried by the center column, V_{flex} , is not easily made. It is not possible to compute V_{flex} as q_{flex} times the area bounded by the positive yield-line and the column periphery due to the presence of shears and twisting moments along the positive yield-line. Attempts to compute nodal forces using Johansen's theory (12) proved inconclusive. Hence it was necessary to utilize empirically obtained data in computing V_{flex} .

Plots of percent of total load carried by the center dynamometer made during the experimental phase of the study showed that the percent tended to decrease slightly with increase in load. The

decrease was never more than 5% between first load and failure in shear. In computing V_{flex} , it was assumed that the percent of total load carried by the center dynamometer at failure in shear would have remained constant until failure in flexure. Thus V_{flex} was easily calculated as

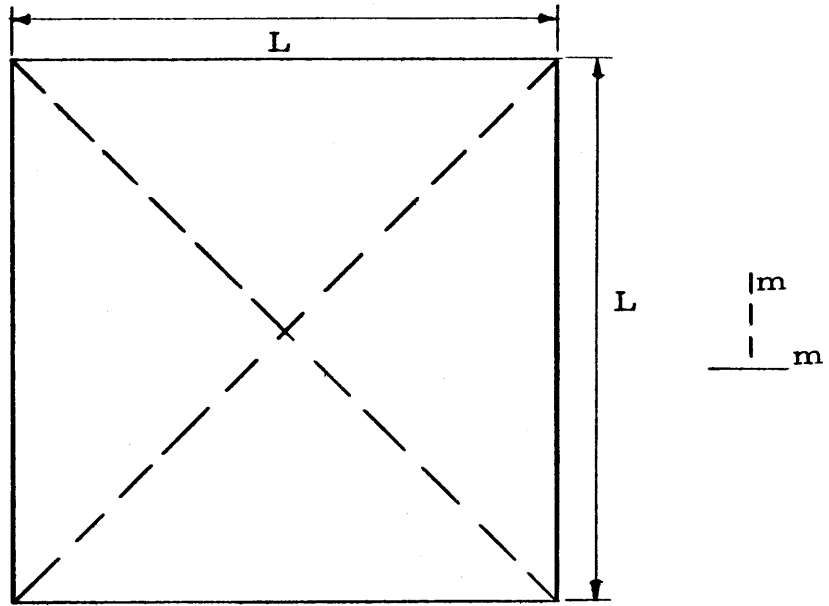
$$V_{flex} = V_u \frac{q_{flex}}{q_{test}} \quad (A12)$$

| i | Q_1 | Q_2 | Q_2/Q_1 |
|---|-------|-------|-----------|
| 1 | 3.73 | | .95 |
| 1 | | 3.53 | |
| 2 | 4.5 | | .96 |
| 2 | | 4.31 | |

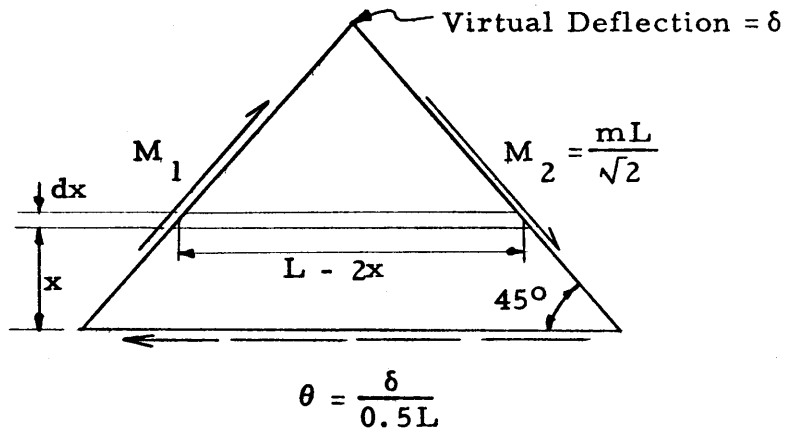
$$Q_1 = \frac{qL^2}{6m} \text{ (without corner levers)}$$

$$Q_2 = \frac{qL^2}{6m} \text{ (with corner levers)}$$

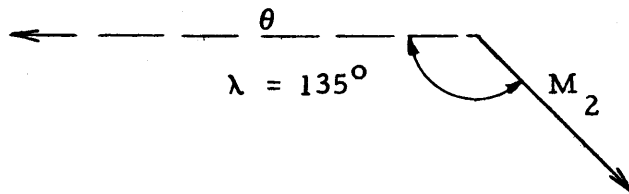
Table A. 1. Comparison of Analyses with and without Corner Levers



a) Slab With Yield Line Pattern



b) One Quadrant With Moment and Rotation Vectors



c) Moment and Rotation Vectors

Fig. A. 1. Yield-Line Analysis of Uniformly Loaded Simply Supported Slab

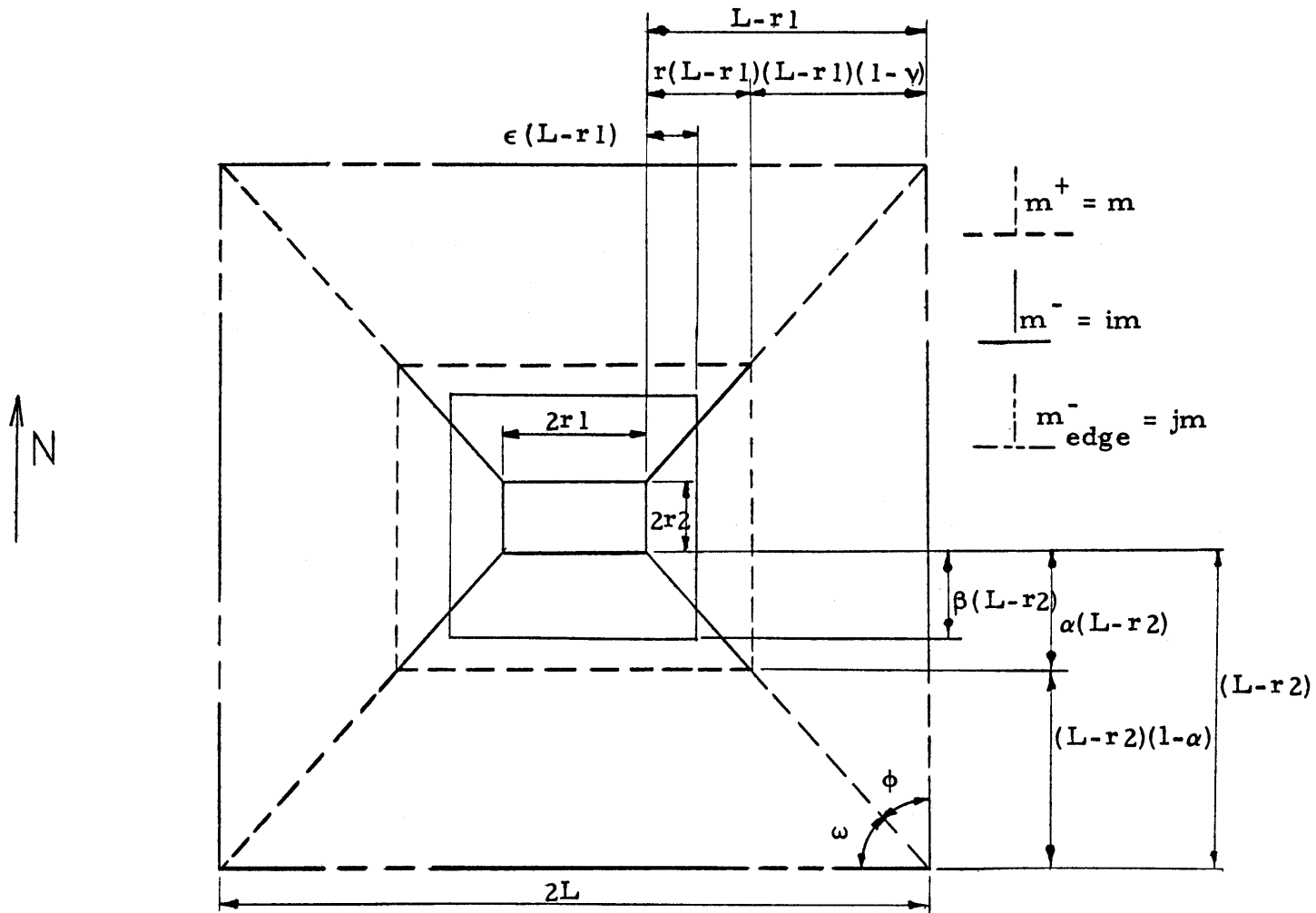


Fig. A. 2. Yield Line Pattern

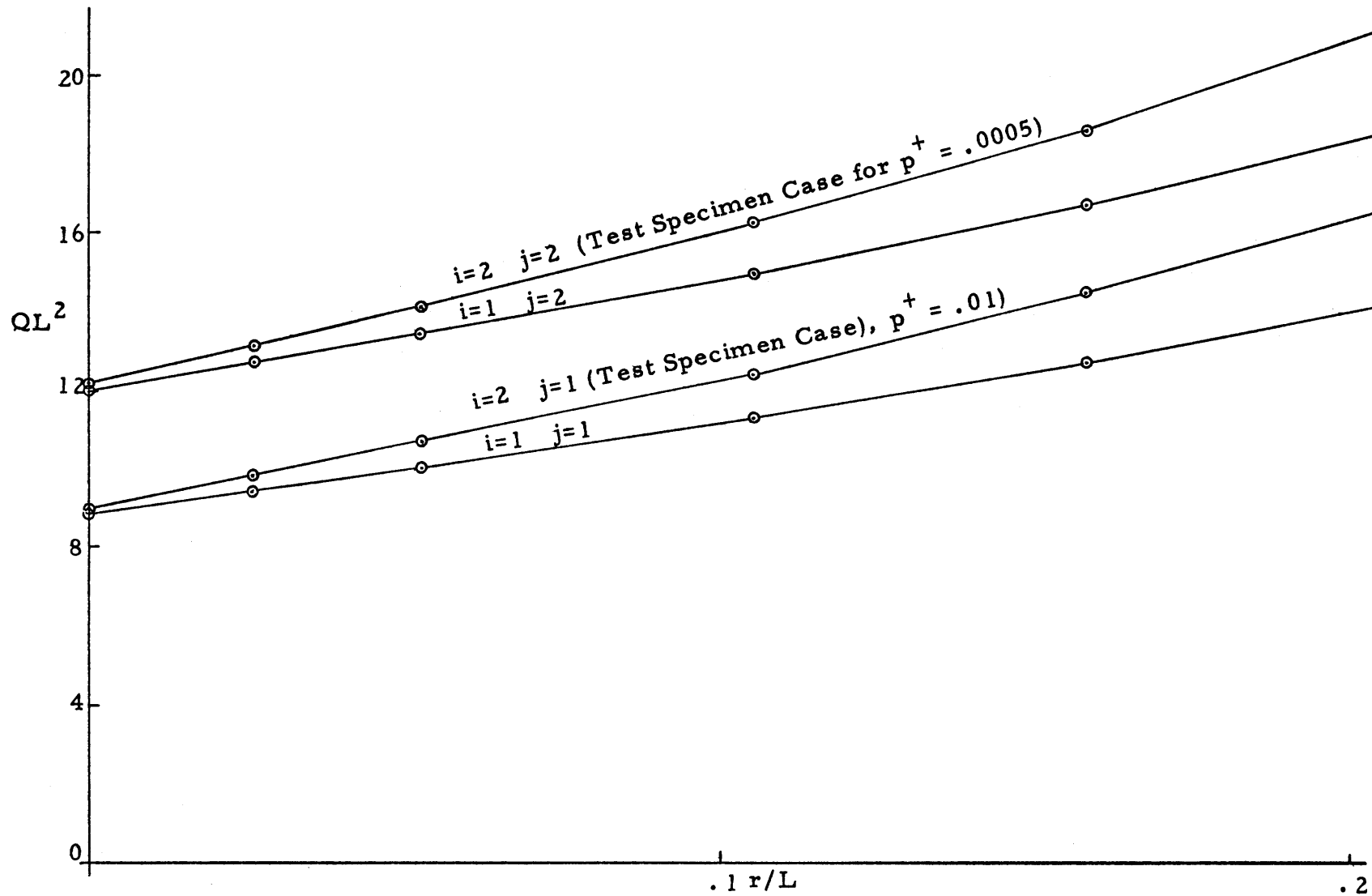


Fig. A. 3. Variation of QL^2 With r/L

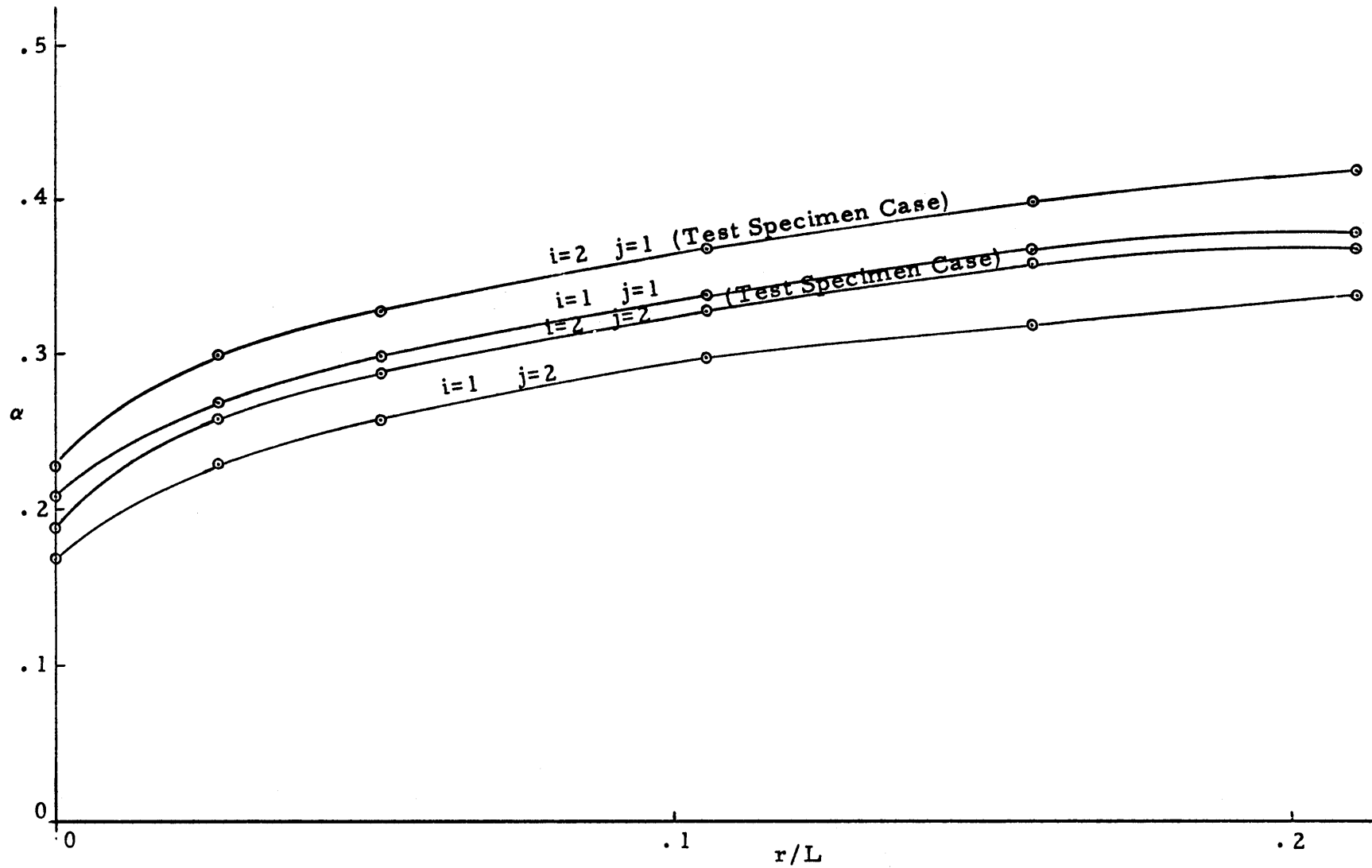


Fig. A.4. Variation of α With r/L